FACULTY OF SCIENCE
UNIVERSITY OF COPENHAGEN

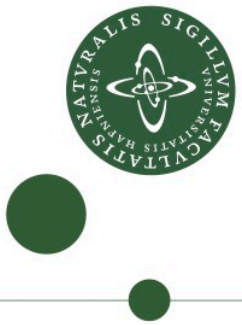

Master Thesis

Emil Tolker-Nielsen Cortes

Astrometric Selection of Quasar Candidates From Gaia DR2

The Niels Bohr Institute

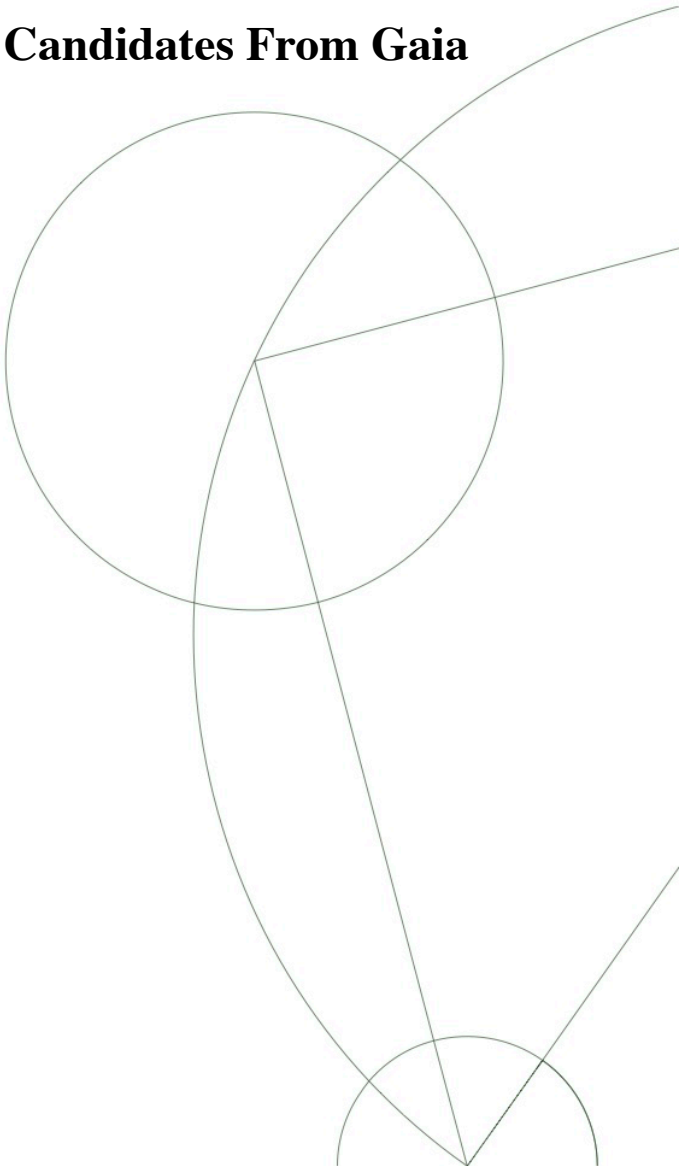

Supervisor: Johan P. U. Fynbo
September, 2019

Abstract

We use European Space Agency Gaia mission second data release, combined with a known Quasar Catalog extracted from SDSS, UKDISS and WISE surveys within the area of strip 82.
First, the astrometric data of the Gaia mission is checked for all the known quasars in our catalog. Within the accepted error, only 12 objects among the 3517 turn out to have significant proper motion. After verification, 10 are confirmed quasars, and one is a star. A particularly high proper motion quasar is worth further studies as we can't explain this high proper motion.
Second, we observe all sources within strip 82 and use color magnitude added to zero proper motion to create a quasar candidates table. We used the WISE band as it is the cleanest selection band. From an initial 554496 Gaia sources we select 1931 in our quasar candidates catalog.
A step further to this thesis would firstly be to observe the particular quasar in order to understand why it has such high proper motion, and secondly to observe the quasar candidates in order to test the efficiency of this selection technique.

Acknowledgement

I would like to thank my master thesis supervisor, Johan P. Fynbo, that allowed me to pursue in my project to become an astronomer. His guidance and patience helped me to work through this thesis.

I would also like to thank my wife for the support and encouragement she gave me through all the process of this thesis.

And finally I would like to thank my family for always being there for me.

Contents

Chapter 1

Introduction

1.1 History

Quasi-stellar radio sources/objects called Quasars have long been observed by astronomers, many have been stored in catalogs as stars before they were discovered as quasars, hiding their true nature. The discovery of quasars and radio galaxies has been the engine in the development of radio astronomy. All the research began with the detection of a weak radio signal coming from the Milky Way (MW) detected by Karl Jansky [9](1935), and the creation of the first amateur radio telescope by Grote Reber in the 1930's, mapping two main radio sources known as Cyg A and Cas A. Two amateurs began a search that would lead to a whole new field of astronomy. Even if it took long for optical astronomers to get any interest in radio astronomy, the development of radio telescope took off in the late 1940's and 1950's in England and Australia with the creation of Astronomical interferometers. When radio image resolution became high enough to compare the results with optical observation, it was though that the radio waves from Cyg A were coming from the collisions of 2 galaxies. Later, with better resolution, it was found that it was not coming from a "collision" but from two gigantic lobes of 200 000 light years. The energy of these lobes would come from a unique super massive black hole.
These new radio galaxies convinced American universities to invest the radio astronomy field. In 1960, Allan Sandage received the radio image of the very small radio-source 3C-48 measured by Tom Mathews. Sandage observed the source with the Palomar telescope (the largest optical telescope at that time) and was very surprised not to find a galaxy but just a small blue star (Matthews and Sandage, 1963 [14]). After observing the spectra of this

supposed star, he described it as the strangest spectra he had ever seen. The lines were not identified and he just didn't know what this object was. Several similar objects were found during the following years.
In 1963, Maarten Schmidt saw on his spectra of 3C-273 that the strong lines he was observing were actually the Balmer transitions lines but very shifted (16%), nobody had seen such redshift before (Greenstein, J. L., Schmidt, 1964 [7]). The study of the 3C-48 finally gave magnesium and oxygen lines, shifted 37%, meaning the two objects were then at respectively 2 and 4.5 billion light years from us. But such far distance and such luminosity leads to a confusing conclusion, their luminosity must be hundreds of times the luminosity of the brightest known galaxy, so definitely not a star. Even more confusing, the study of 3C-273 flux variability showed that it is "1 light month" wide (Smith, H. J., Hoffleit, D.,1963 [21]), when a standard galaxy can be 100 000 light years, for a luminosity 100 times smaller. Many theories came out to explain this luminosity but the only a few were very plausible, the main one being a super massive black hole(SMBH) in the center of a galaxy (Salpeter, 1964 [18]. To support this conclusions, astronomers required the help of theorists. For the first time all branches of astrophysics worked together on a same subject.
In 1965 it was discovered by Sandage that some quasars were radio quiet, and that quasars had lots of similarities with the closer to us Seyfert Galaxies (spiral galaxies with an intense luminous center). Together they form the Active Galactic Nuclei (AGN) family. Since the beginning of the observation of quasars it as always been obvious that these object sending us early images of our universe were to observe and to study very carefully.
Studies still argue if radio loud and radio quiet quasars form a Unified model of quasar, this will be discussed in section 1.3.1. All quasars are being, without any doubt powered by a SMBH accreting mater, the energy source being the gravitational potential of the central black hole. AGN have specific characteristics proper to themselves. In the core of the AGN there is a SMBH, surrounded by its accretion disk that powers the whole system. Next to this accretion is the Broad line region (BLR) and surrounding it are the Torus and the Narrow line region (NLR). Two jets are emitted in opposite direction, they can be more or less powerful but all jets show relativistic photons spiraling in a magnetic field, and when these charged particles are accelerated they radiate photons at radio wavelengths, this effect is called synchrotron radiation (see Bradley M. Peterson,1997 [16]). The structure of quasars will be discussed more in detail in the following sections.
The detection of quasars is, to a large extent, determined on the position we

observe it, if we observe directly the jets, we would see a radio excess and a great variability that would describe a Blazar (BL objects), observed from other parts would lead to seeing quasars, that can be radio quiet or radio loud depending on the specific object. A radio loud quasar would come from an AGN with strong radio lobes and jets, when a quasar with a low intensity jet would rather be radio quiet. A brief overview can be seen in figure 2.1 and this will be re-discussed in section 1.3.

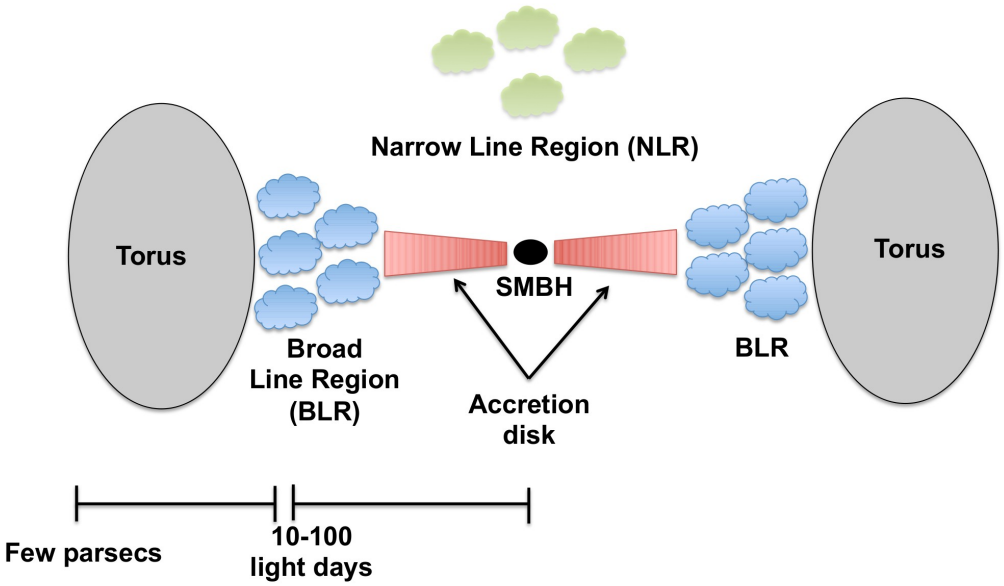

Figure 1.1: A schematic illustration of the currently favored model for how quasars are structured (http://www.isdc.unige.ch/ ricci/Website/Active_Galactic_Nuclei.html)

1.2 The quasar phenomenon

1.2.1 Variability

One of the most noticeable proprieties of quasars is its variability in all wavelengths (e.g., Smith and Hoffleit 1963 [21]). The variation can last from a few months to days. This period gives an idea of the dimension of the nucleus as of course the region, due to causality, must be smaller or

equal to light travel distance in the variability time scale. This leads for a quasar with a period of days to a length of 26 billion kilometers, which is comparable to the size of the solar systems. So a quasar is emitting 100 times as much energy as an entire galaxy, in a size comparable to the solar system. This intense luminosity is based on the supposed distance of the quasar derived from the redshift.

1.2.2 Eddington luminosity

The Eddington luminosity is the maximum luminosity an object can have before breaking the balance between radiative forces and gravitational forces. It gives very important information's about quasars, as their luminosity is so high, the Eddington limits allows us to derive important parameters such as mass. Assuming the stable isotropy of a source, it is possible to derive a minimum mass from the Eddington limit given by

$$M_E = 8 \cdot 10^5 L_{44} M_\odot \tag{1.1}$$

with L_{44} the central luminosity in units of $10^{44} erg \cdot s^{-1}$. The typical quasars luminosity would be $L_{QSO} \approx 10^{46} erg \cdot s^{-1}$, resulting a central mass larger then $M_{QSO} \approx 10^8 M_\odot$ is required. From this we can derive the Eddington luminosity as:

$$L_E = \frac{4\pi G c m_p}{\sigma_e} M \tag{1.2}$$

which gives us the maximum luminosity an object of mass M can have. These results allow us to tell that quasars are from the size of a solar system but with a mass of around millions, to billions times the solar system mass and emitting much more energy than galaxies. It is difficult not to imagine that it is a black hole that powers this mass (Salpeter, 1964 [18] and Zel'dovich, 1964 [28]) and nearly every astronomer supports this theory.

1.2.3 Ultraviolet fluxes

As said in last sections, the first look on a quasar by Allan Sandage (1965[19]) looked like a blue star. When we look at the UVB photometry, it shows that $U - B$ is very small and is referred as an ultraviolet excess, but this is only relative to the spectral energy of stars. Quasars basically appear blue because their spectra is flatter then spectra of stars through the U and B band.

This specificity leads to a detection technique using UVB magnitudes, using the $U - B < 0$ as a selection criteria.

1.2.4 Red-shift

A very important measurement to understand the real nature of quasars is of course the redshift measurement. The redshift is a quantity defined by the observation of a spectral line, which would be shifted from its laboratory position and derived as following:

$$z = \frac{\lambda - \lambda_0}{\lambda_0} = \frac{\lambda}{\lambda_0} - 1 \tag{1.3}$$

In the frame of the expansion of the universe, the red shift gives us an idea about the speed of the object, and the time light takes to come to us. Thanks to cosmological models, it is possible to derive the distance between us and quasars. A large frame of different redshifts as been collected from different quasars, from redshifts around z=1 to the highest redshift to be z=7.54 (Bañados et al., 2018 [1]). First consequence of this high redshift is the deduced luminosity of quasars. Second is to see absorption lines in the spectra that have different redshifts (lower) which come from objects in the path of the quasars light and then act like a probe, this will be discussed in part 1.3.4.

1.2.5 Accretion disks / fueling of quasars

As discussed in last section, quasar are some of the most power full object in the univers. They have extreme luminosity, but the very interesting parameter is the variability of quasars. This variability is a chance for astronomers to measure the size of the central part. The size of quasar would be the distance light travels during one variability. Typically quasars are few light days long. So the question would be how an object of the size of the solar system can be as luminous as hundreds of galaxies without exploding? Of course the first idea is to imagine a super massive black hole in the center, of at least $10^6 M$, that would counterbalance the radiative energy. The high luminosity is then explained by the accretion disk.

1.3 Quasar and AGN - a unified model

Quasars belong to the Active Galactic Nuclei (AGN) family together with Seyfert galaxies, Blazars and to some extent radio galaxies. They all possess an intense and powerful nuclei driven by the SMBH in its center. Seyfert galaxies are not as luminous as quasars, and their host galaxy can be directly observed which is impossible with quasar for whom the intense luminosity overwhelms the center making it impossible for us to observe. Seyfert Galaxies have typically lower redshifts than quasars, even if some exceptions have been observed.

1.3.1 Radio Loud Radio quiet

Quasars, and AGN's in general are divided in two main family, radio loud and radio quiet. Radio emission is the first clue that led astronomers to discover quasars, and a very important figure is when it was discovered that quasars are not necessary radio loud (Ryle, M., Sandage, 1964 [17]) and it is thanks to the development of a new selection technique involving U magnitude excess (discussed in section 1.2.3). The main reason why some QSO's are radio loud and some radio quiet is due to the presence of radio lobes coming from the jets expelled by the center of the source. All quasars have jets but the intensity of their emission can be very variable, leading to some quasars having very strong radio figures and other with very weak ones. The intensity of a jet is directly correlated to the SMBH in the center of the source, as the strength of the jet emission depends on its spin. If the SMBH spins fast, the jet would be strong and and we would observe a radio loud quasar, in the other hand if the SMBH spins slowly, it will produce weak jets and we would see a radio quiet quasar (Wilson and Colbert 1995 [25]). Radio quiet is an exaggerated name as almost all radio quiet quasars have very weak but existing radio fluxes, but there is a very large gape between the emission strength of radio loud and radio quiet QSO's that justifies this appellation. This large gape is a mistery for astronomers, but this is out of the scope of this thesis. A particular case of radio loud quasars would be observed if the object is directly observed through the jets axis, known as radio axis. in that case we would talk about a Blazar that has the particularity to be very variable and with a very large radio emission.
Some papers stat that maybe low spinning of the SMBH could lead the galaxy hosting radio quiet quasars to be more efficient in star formation, enhancing the idea that radio loud and radio quiet quasars are two distinct

populations (Zakamska, Nadia L., et al. 2015 [27]).

1.3.2 Broad line region

The Broad line region (BLR) is the closest region surrounding the SMBH after the accretion disk. As its name lets it understand, this is a particular region that produces very broad emission lines. Broad emission lines are a dominant figure of many AGN's spectra, so it is a common phenomenon for all Quasars. The emission lines are believed to be driven by photoionization by the central source and most of the recombination emission originates in the broad line cloud that is optically thick. The high density of the BLR makes forbidden lines collisionally suppressed and thus impossible in this region (B.M,Peterson, 1997 [16]).
The main interest in the study of the BLR is the ability to map the inner part of the AGN. In the case of quasar it is of major importance since we can't observe the inner part of the source. the technique used is called reverberation mapping. This is out of the scope of this thesis, but the interest in it is great as it allows to estimate the mass of the central SMBH and its size.

1.3.3 Narrow Line Region

The Narrow Line Region (NLR) is a vast region around the central source, that can be illustrated like a cloude around the central part and the dust torus. This region produces Narrow lines in the QSO's spectra. The ionizing radiation coming from the central source dominates in this region and the electron density is low enough to produce forbidden lines, which helps us to estimate and measure main parameters of the NLR gas such as electron density and temperature.
A typicalevalue for the NLR gas Temperature is $T_e \approx 16000K$ (Koski, A. T., 1978 [11]). Some measurement of the mass of the NLR gives the NLR heavier than the BLR, but the BLR being so dense its emission overwhelms the NLR.
An other information the NLR gives us is the description of the kinematics of the gas.

1.3.4 Probes

Quasars are of great importance as they can work as probes of the universe. Until now we mainly discussed the emission lines that quasars could send us, but its is equally or even more important to observe the absorption features that are the keys the mapping of the universe
If the quasar is not to much redshifted regarding the beam of the instrument, it may be possible to observe the Lymanα line and the Lyman forest. The Lyman forest is a great way to understand and measure what the light of the quasar encountered on its path, and thus is important to understand.
Absorption lines can also be observed, if they come from an object on the path of the quasar, the absorption line will be redshifted differently then the quasar redshift, then by identifying the source, we can set that the object is at such distance from us and continue our mapping of the universe. This mapping is of great use to understand how and when Galaxies and stars form.

1.4 Quasar identification

As seen before, the study of quasars is essential to deepen our knowledge of the universe and galaxy/stellar formation. But quasars are difficult objects to detect as they can optically look as stars and also that quasars are very faint objects. A pre-idfentification of candidates is necessary and then must be verified by their spectra once selected.

The first identification technique resulted from quasar discovery and consisted on matching star like object positions and radio source position. Stars would not radiate in radio wavelengths so it has been understood that the objects were quasars. Very rapidly it was also understood that all quasars do not radiate radio wave (around 10% actually radiate in radio wavelengths) and thus this identification technique had to be changed. Soon it has been understood that stars and quasars have different optical UVB color diagrams (Sandage, 1971 [20]). The SED of stars being well known and temperature dependent, the blue color of quasars would deviate the track they follow from the stellar diagram ($U - B < 0$). The only problem is that some of the most effective color identification turned out to be very contaminated by galactic stars and only 5,4% of candidates resulted being quasars (Green and alt, 1986[6]).

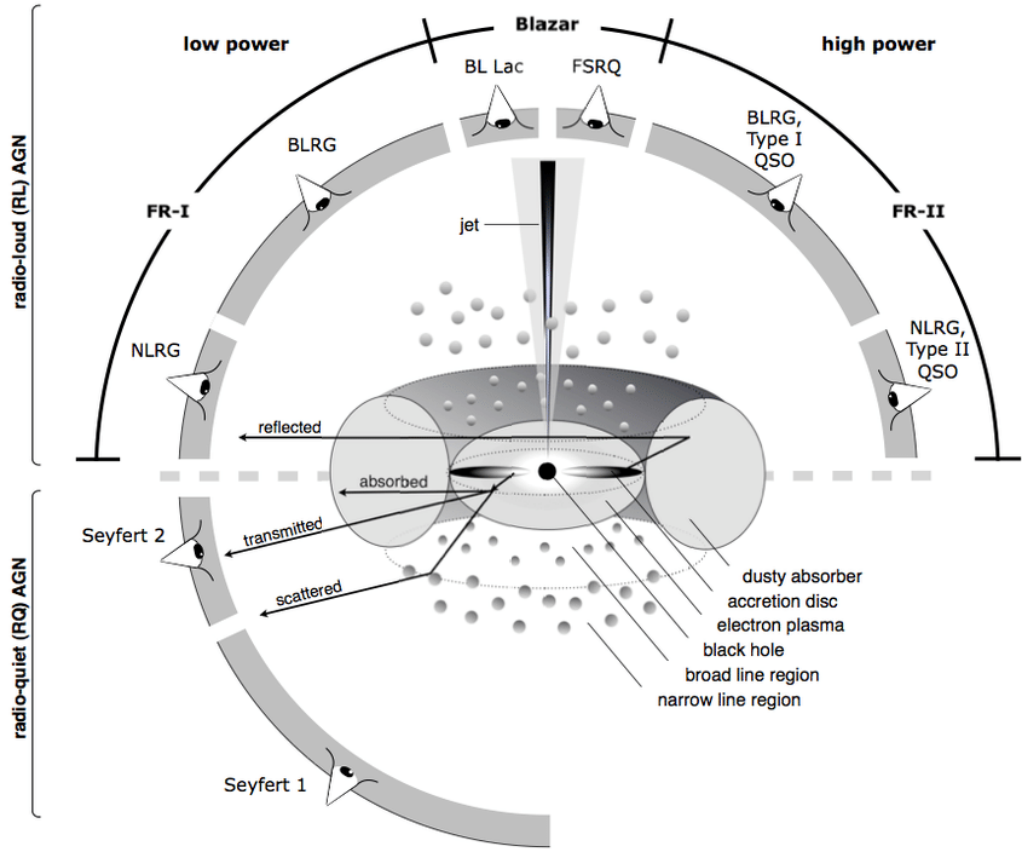

Figure 1.2: Unified model of AGN. Image credits Britto, R. J.,2002 [2]

Historically the next detection technique would be introduced by Low and Kleinmann (1968 [12]) emitting the possibility of observing the infrared radiation coming from the hot torus. It is only two decades later than the technically challenging process to do so was set by building the Infrared Astronomical Satellite (IRAS).

As Ultraviolet fluxes selection was found to be very biased by stellar population, studies focusing on infrared selection where discussed (Low and Kleinmann 1968). The technological and understanding of using infrared as selection technique was a challenging problem and it took two decades to reach to some results. Many different surveys were tried such as de Grijp et alt (1987). The use of Near infrared (NIR) as been developed to avoid contamination by dust, as NIR is less affected by dust reddening. Similarly then

with UV excess, one of the most recent technique as been based on the observation of the K-band. In the same way as with $U - B < 0$, the J-K band appears very different for quasars then with stars, which provides a very good technique to discriminate stars from quasars, but unfortunately galaxies have similar J-K band, which shifts the problem from stars to galaxies. Other infrared surveys have been used such as Mid-Infrared (MIR) survey (Wright, et al., 2010 [26] and Stern et al, 2012 [23]) and other using 2 MIR surveys (Mateos et al, 2012 [13]).

Some other search were also based on other proprieties of quasars, such as variability (Usher and Mitchell 1978[24]) and of course X-Ray detection (Grazian, A., et al,2000[5]), as it is one of the only propriety shared by all quasars. It has even been made by Serendipity (McCarthy et al. 1988 [15]).

The identification criteria that is applied in this thesis is using astrometry, considering that Quasars are stationary sources. This idea was already emitted in the 1980's (Koo et al. 1986 [10]) but was impossible to apply with the technical progress at that time. Thanks to the ESA Gaia mission it has been made possible to use this technique that as a great potential to identify with more efficiency Quasars and even maybe find new types of Quasars.
My research for zero proper motion sources is the direct continuation of a previous work of my supervisor Johan P.Fynbo co-wrote (K.E.Heintz,2018 [8]). This work is focused on quasar identification using zero proper motion within an area of 1 degree around the galactic north pole. This research led to a great efficiency selection within high latitudes, as only $\leq 25\%$ of selected sources were not identified as quasars. My research is very similar to this but I extent it to a larger survey in the sky.

Chapter 2

Gaia satellite

The Gaia mission is an European space agency(ESA) mission launched in 2013 and expected to last until 2022. Specialized in astrometry, Gaia follows the legacy of the previous astrometric ESA mission Hipparcos, also specialized in astrometry. Gaia aims to touch a larger amount of sources compared to Hipparcos. The astrometry data is divided on two subsets, a 2 parameter astrometric solution with standard right ascension and declination (361 009 408 sources) and a 5 parameters astrometric solution that adds parallax, and proper motion regarding right ascension and declination (1 331 909 727 sources). Typically the 2 solutions objects are the very faint object with Magnitudes $G > 21$.

The space craft is composed of two telescopes separated by a wide angle of 106.5 degrees, the space craft would rotate around an axis perpendicular to the telescopes line of sight.
This system will allow the telescope to observe each sources at least 70 times during its lifetime, this continuous observation allows a good observation time and gives us good measurementts of object within the milky way and beyond. Gaia allows us to observe very faint sources for the first time, sources that were too faint to be detected in previous missions. Quasars being faint sources, the Gaia telescope gives us a great opportunity to observe new sources and specially hope to see new quasars. But with observations and instruments always comes uncertainties. This uncertainties on Astrometry are different regarding the magnitude and are described in the following table 2.1 :

Table 2.1: Basic performance statistics for Gaia DR2.

Data product or source type	Typical uncertainty
Five-parameter astrometry (position & parallax)	0.02–0.04 mas at G 15
	0.1 mas at G = 17
	0.7 mas at G = 20
	2 mas at G = 21
Five-parameter astrometry (proper motion)	0.07 mas yr^{-1} at $G < 15$
	0.2 mas yr^{-1} at $G = 17$
	1.2 mas yr^{-1} at $G = 20$
	3 mas yr^{-1} at $G = 21$

2.1 Proper motion estimation

Gaia gives us one of the largest catalog of astronomical sources, specially stars of our galaxy, its outstanding precision and amount of objects it observes, makes the use of its data interesting too all branches of astronomy, and allows us today to search for quasars thanks to astrometry. The Gaia data is made fully available to anyone, unlike the Hipparcos mission, and we have used data from the second data release of the mission. The main aim of the thesis is to try to isolate quasars thanks to proper motion measurement delivered by Gaia.

A quick calculation of quasar maximum proper motion regarding different redshifts ranges can be made. Taking the maximum velocity it could have is the speed of light (which would be highly surprising), and the direction it would be perceived the fastest for the observer would be a direction perpendicular to the line of sight. Knowing this, we can calculate the maximum proper motion a quasar would be supposed to have, regarding its redshift. This results have been stored in Tab 2.

As shown in the table the proper motion is nearly around zero for milliarcseconds per year, which is insignificant for observations. And if we rise the redshift, the proper motion will decline more. So Quasars should be objects with zero proper motion and selecting them in that way could be a great possibility to create unbiased catalogs of quasars, that are very difficult to produce for now.

Table 2.2: Tab.2 Theorical Calculation of proper motion of Quasars

redshift	velocity	1 arcsec	Proper Motion
z=0.5	c	6.3 kph	0.049 mas/yr
z=0.5	500 kms^{-1}	6.3 kpc	$8.112e^{-8}$ mas/yr
z=1	c	8.2 kpc	0.037 mas/yr
z=1	500 kms^{-1}	8.2 kpc	$6.232e^{-8}$ mas/yr
z=2	c	8.6 kpc	0.036 mas/yr
z=2	500 kms^{-1}	8.6 kpc	$5.942e^{-8}$ mas/yr
z=3	c	7.9 kpc	0.039 mas/yr
z=3	500 kms^{-1}	7.9 kpc	$6.468e^{-8}$ mas/yr

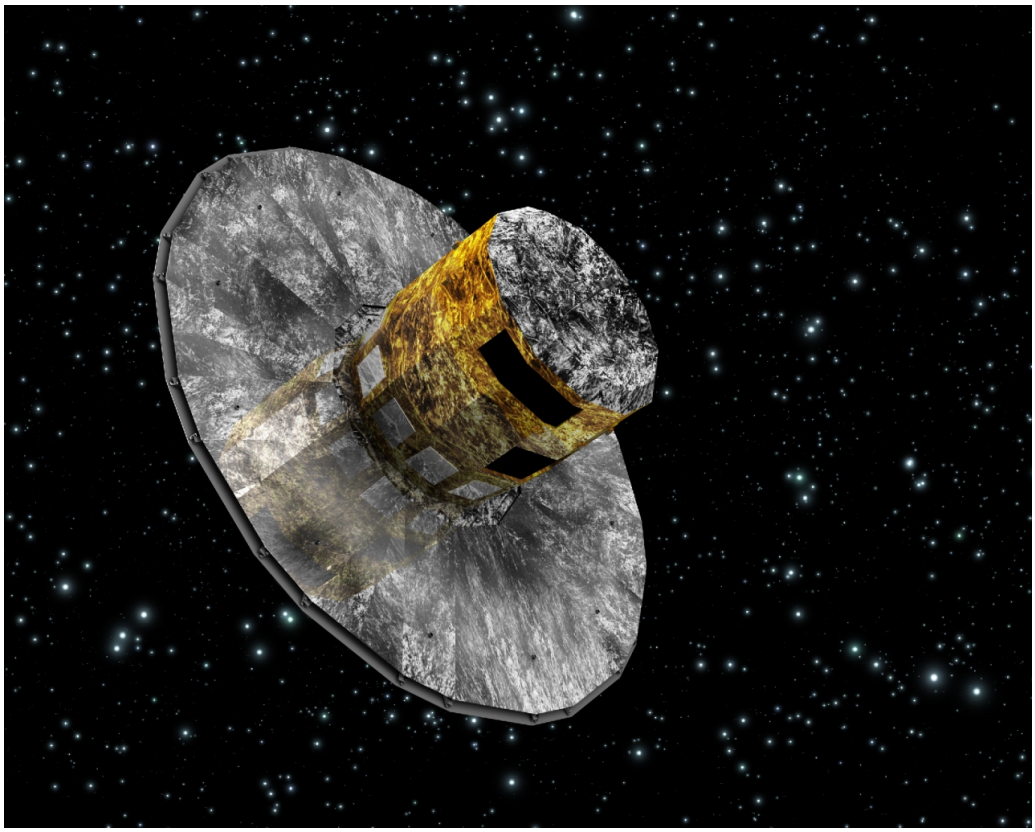

Figure 2.1: Gaia Spacecraft. Artist view, Credit: ESA

Chapter 3

Data selection

Quasars are without any doubt some of the most powerful objects in the universe, as explained in Chapter 1, they are so powerful and bright that they can be measured at very large distances, giving us the opportunity to observe early galactic ages, essential for a better understanding of galaxies and stellar formation. Without any doubt observing Quasars brings us back in time, but the light we receive from this super powered objects travelled millions to billions of light years, finding on its path dust clouds, stars, galaxies, or anything in the way toward us. This light would of course be affected by these encounters and the background light of the quasars turns into a probe of all the universe between it and us. This particularity is without any doubt one of the most powerful tools to map our universe and be able to understand galaxy formation and Black hole formation.
But if thanks to Quasars spectra we can probe all these amazing features with more or less efficiency, finding Quasars isn't something easy, worse is that they hide behind optical blue star shape. Before observing quasars, we have to select them. Their have been many different ways to identify quasars candidates through the decades since quasars were discovered (only 60 years ago) and these techniques were often driven by the instrumental technological advancement.
Today the Gaia telescope gives us a great opportunity to use one of the selection techniques that was long submitted (Koo et al. 1986 [10]) but had not enough technological precision to be realized. Even if the main mission of Gaia isn't quasar observation, it's very precise astrometry measurements is from great use for quasar selection. As said before using zero proper motion for Quasar selection may be from a great use in order to realize large unbiased catalogs of quasars, as it would use a specificity of all quasars,

unrewarding their radio excess, or if they were reddened by dust. The only real parameter shared by all quasars would be their X-ray emission and their ultraviolet flux, but these techniques often turn out to be very biased by stellar populations.

This thesis will be divided in three different main parts. First it will focus on verifying if the Quasar catalog respects the zero proper motion hypothesis. To be considered as being a zero proper motion object, the source must have its error within the 3σ error limit. Then we will focus on how the proper motion correction could very efficiently clean the stellar contamination within color magnitude plots. And in the last part we will discuss the efficiency that can be hoped for this selection technique and create a large catalog of new quasar candidates.

3.1 Data

Quasar candidates were selected based on astrometry and color selection. Data catalogue was based on Gaia mission, astrometry and photometry were based on several surveys, the Sloan Digital Sky Survey (SDSS) for the optical (Eisenstein et al.,2011), Infrared Deep Sky Survey (UKDISS) for the near infrared (Warren et alt., 2017) and the Wide-field Infrared Survey Explorer (Wise) for the mid infrared (Wright et al.,2010). The SDSS photometric data consists of magnitudes in the u, g, r, i, z optical bands at the effective wavelengths 3543Å, 4770Å, 6231Å, 7625Å and 9134Å, respectively. The UKIDSS photometric data at NIR wavelengths are given in the four Y,J,H,K bands with effective wavelengths of. The WISE survey provides photometric data in the MIR in four bands with effective wavelengths 3.4, 4.6, 12 and 22 μm, which later will simply be referred to as W1, W2, W3 and W4, respectively.

3.2 Stripe 82

The selection was made on a well known part of the sky called strip 82. This area covers 300 deg^2 near the equator in the southern Galactic plane that covers from 300 deg to 60 deg in Right Ascension (RA) and from -1.26 deg to 1.26 deg in Declination (DEC). This area is very well known and has been observed several times (scanned 70-90 times by SDSS), it is considered that almost all quasars have been observed in this area and thus it is a good area

to investigate if astrometry is a good tracer for quasars. A celestial overview of all Gaia objects within strip 82 is illustrated in Figure 3.1.
Data has been divided in several categories, in order to discriminate sources, of course we want to separate stars from quasars, but quasars were also divided regarding redshifts. Quasars were separated in such mater because proper motion relies strongly on redshift. Sources with magnitudes higher then 21 have been excluded, considered too faint to obtain proper proper motion measurements.

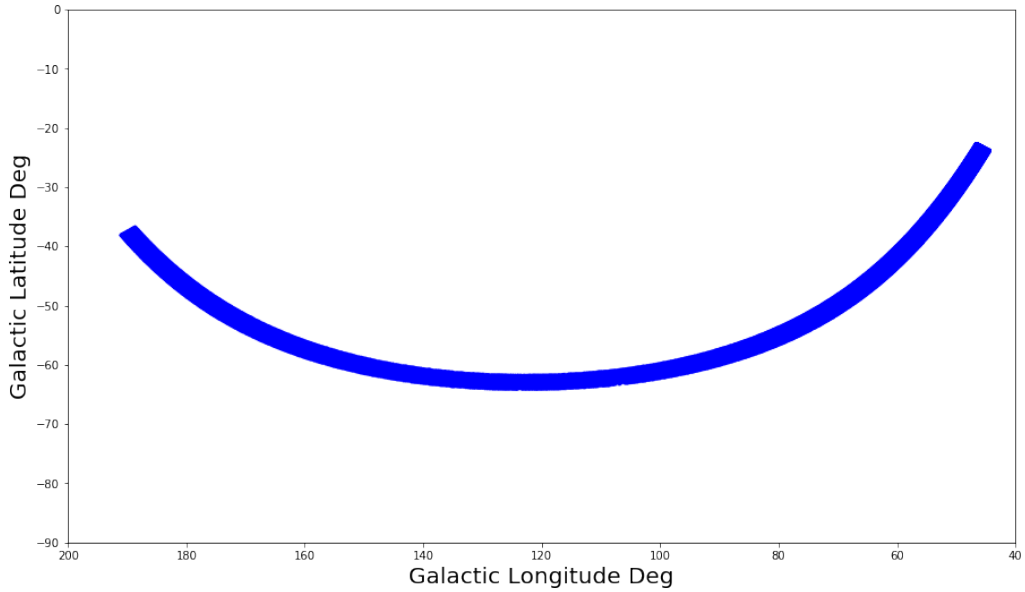

Figure 3.1: All Gaia sources within Galactic coordinates in strip 82

Chapter 4

Results

4.1 Proper motion of known quasars

As discussed in the previous section, I created a data catalogue from several surveys, coming from SDSS, UKIDSS and WISE, all having observed strip 82 several times and giving us a large quasar catalogue, observed by Gaia. This catalogue is filled with 3572 known quasars. Gaia observation gives, as discussed previously, a five and a two parameter data. Proper motion can only be observed in the five-parameter objects. Unfortunately 55 objects from my catalogue fall in the two-parameter selection and thus have no proper motion data for now (maybe the third run of Observations from Gaia will correct these objects).
After removing these 55 objects, I ended up with 3517 quasars in my catalogue with proper motion. The result of the proper motion determination is shown in Figure 4.1. It is very apparent that most QSO's are within the 3σ limit, so almost all quasars are considered to be zero proper motion objects.

Among our Quasar Catalog, 12 of the objects have non zero proper motion and the detail of these objects are shown in Table 4.1 (Stellar coordinates of these sources can be found in Table 6.1 in the appendix).

Most of these objects have proper motion around 3 or 4 σ but three different objects have very high proper motions and need to be discussed.

*S*DSS J010345.56+003746.7

This object has right Ascension of 15.9399 deg and Declination of 0.6296 deg and redshift z=1.164. It can be seen in Figure 4.2 that this object is

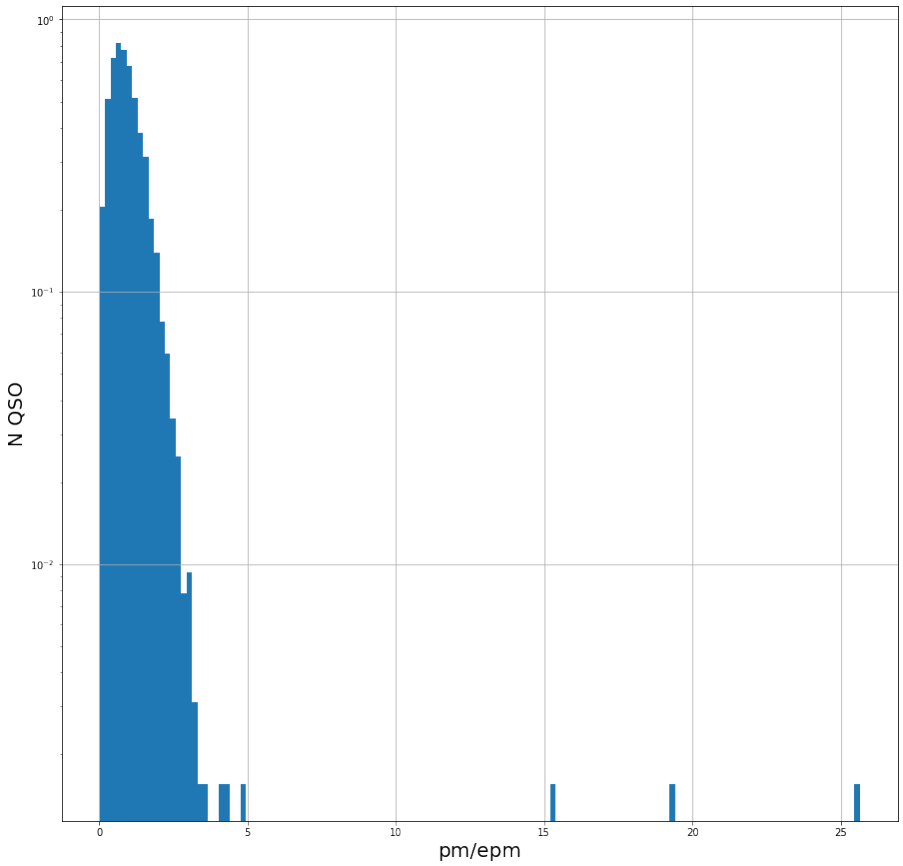

Figure 4.1: Histogram of Quasar population regarding proper motion

a hot blue star, the Balmer bump can be clearly seen around 4000 Å. the image confirms the shape of a blue star and there is no apparent object that could have biased the spectroscopy. This object must have been wrongly classified as a quasar at some point.

*S*DSS J214042.01-004358.7

This object has right Ascension of 325.1751 deg and Declination of -0.7330 deg and redshift z=2.187. The very high proper motion obtained for this objects is without any doubt due to the object in the line of sight that can be seen in Figure 4.3. When focusing the observation on the quasar, we can see a very typical quasar spectra with broad emission lines. new observation with more precise coordinates will be necessary to determine

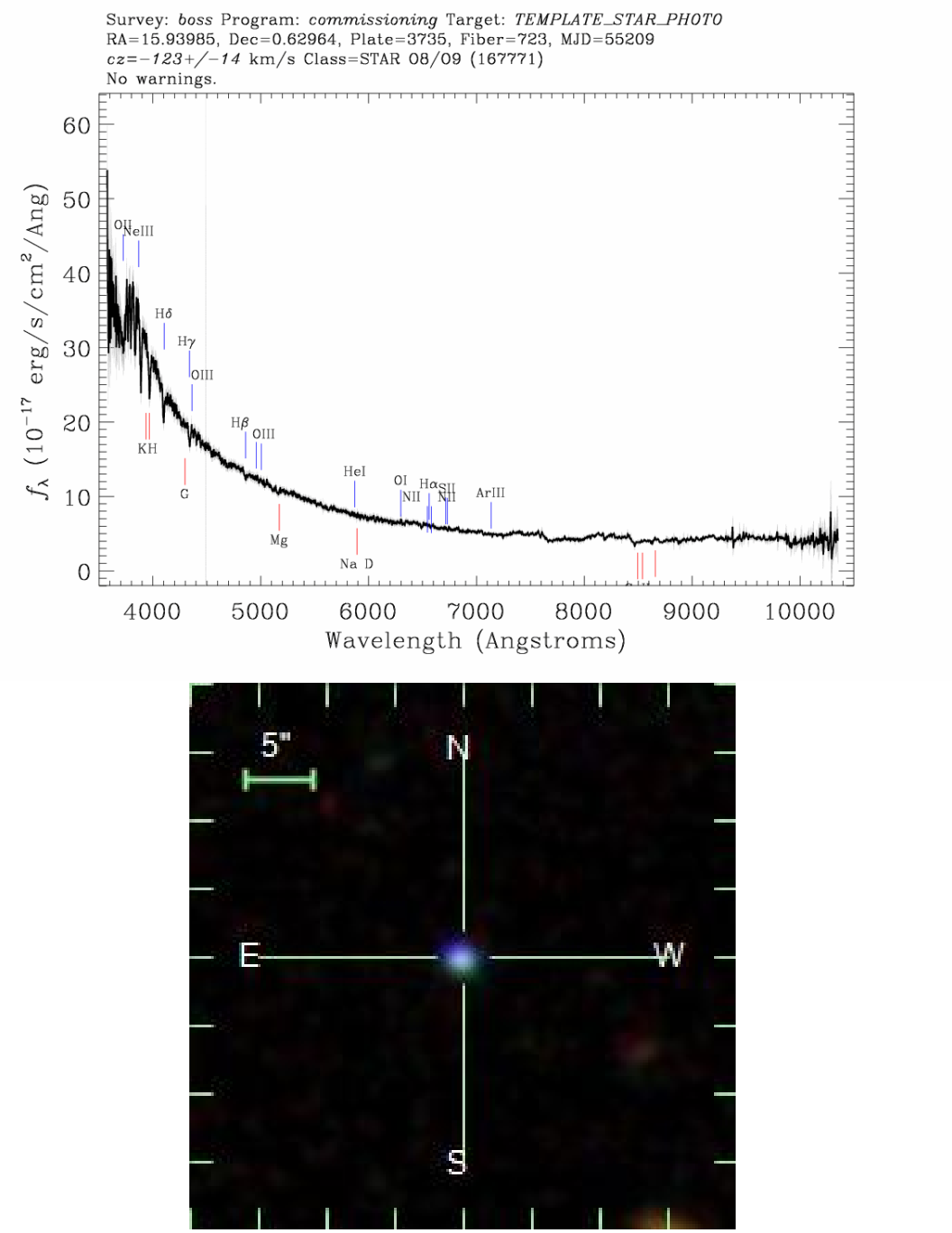

Figure 4.2: SDSS J010345.56+003746.7 Spectra and Overview

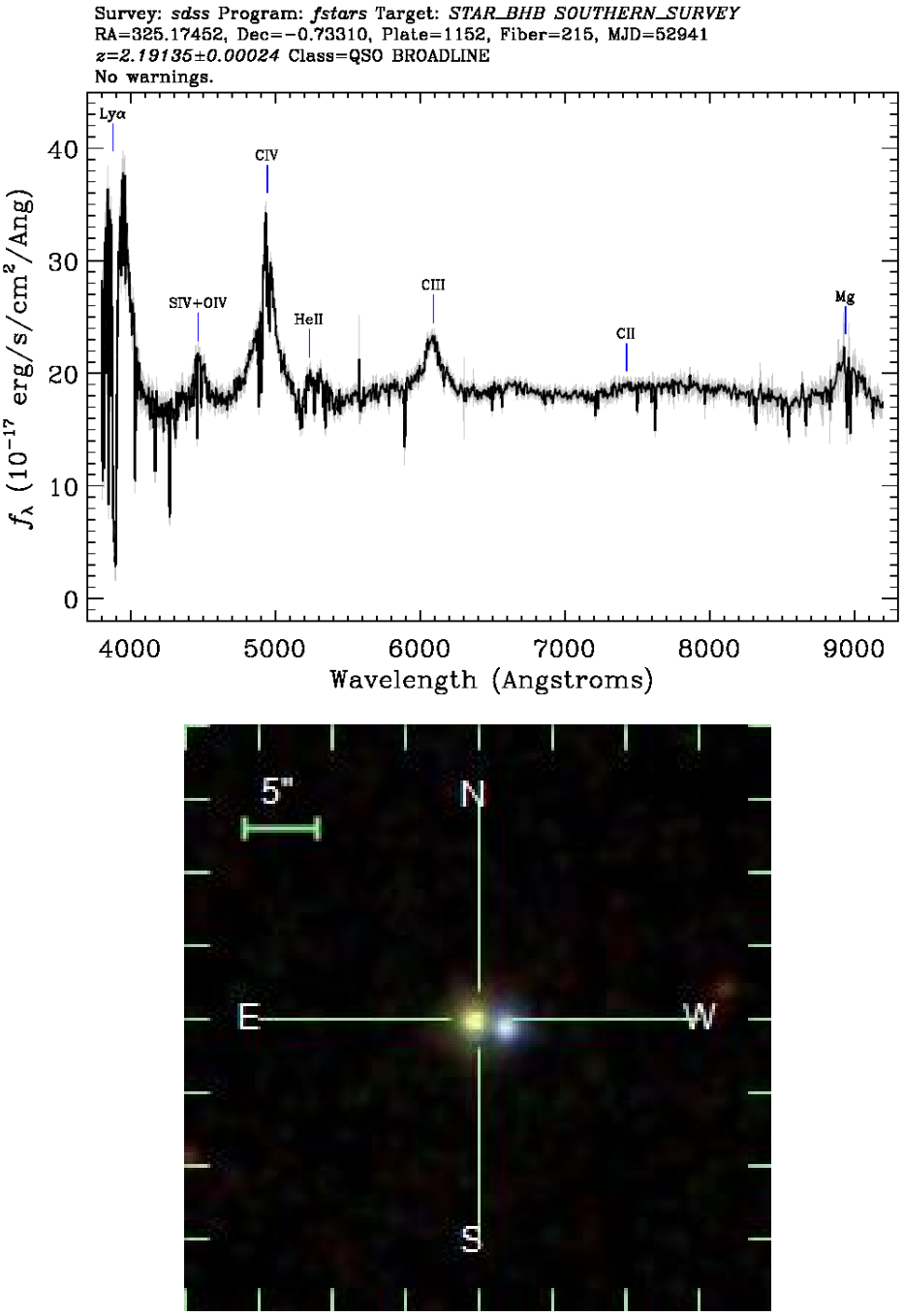

Figure 4.3: SSDSS J214042.01-004358.7 Spectra and Overview
A star in the line of sight must have been the reason of such high proper motion. The spectra is from the individual quasar on the right.

Table 4.1: Non zero proper motion objects list and their theoretical transverse velocities

Name	Proper Motion (mas/yr)	redshift	Velocity (kpc/yr)
SDSS J002516.70+002221.9	3.6676	1.448	3.11×10^{-2}
SDSS J010345.56+003746.7	25.6380	1.164	2.18×10^{-1}
SDSS J013306.18-004523.8	4.2372	0.733	3.18×10^{-2}
SDSS J013446.47-004652.0	3.0220	1.346	2.61×10^{-2}
SDSS J014243.53-002754.1	3.2723	2.735	2.65×10^{-2}
SDSS J022349.72-011347.4	3.3726	1.95	2.29×10^{-2}
SDSS J022723.99-010623.4	19.3624	2.178	1.16×10^{-1}
SDSS J023617.50+002557.6	4.1809	1.502	3.64×10^{-2}
SDSS J025247.33+005135.1	3.0264	2.115	2.58×10^{-2}
SDSS J030501.15+003702.9	3.2286	1.156	2.74×10^{-2}
SDSS J214042.01-004358.7	15.3840	2.187	1.31×10^{-1}
SDSS J230015.18+010520.0	4.8158	1.643	4.19×10^{-2}

the proper motion of this Quasar.

*S*SDSS J022723.99-010623.4

This object has right Ascension of 36.8500 deg and Declination of -1.1066 deg and redshift z=2.178. This is the most intriguing object in our observation. No apparent object could disturb the spectral or astrometrical observation of this object, but looking at the spectra it is very surprising to see that without any doubt, this is a quasar spectra. The apparent velocity calculated for this quasar is 537 times the speed of light, which is way more then the speed of light.

4.1.1 Superluminal motion

Superluminal motion is a phenomenon that appears when an observer sees an object with apparent velocity higher than the speed of light. Of course the actual velocity of that source is not faster then light, this effect is an illusion created by the lobes. This illusion of supraluminal motion is caused by the jets of the object. These jets are coming from the SMBH and have velocities close to light speed (c). But compact cores as quasars are, as we

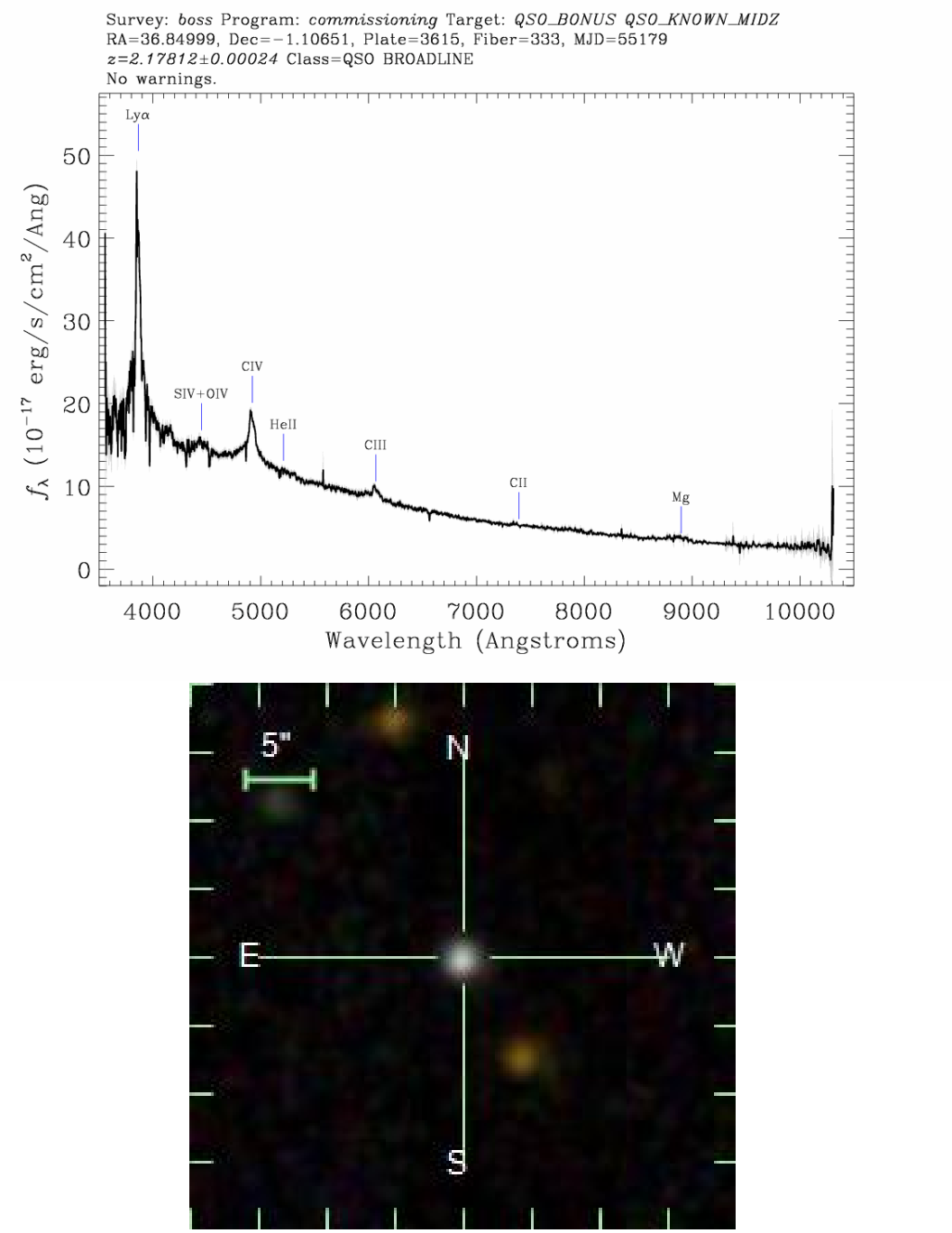

Figure 4.4: SSDSS J022723.99-010623.4 Spectra and Overview

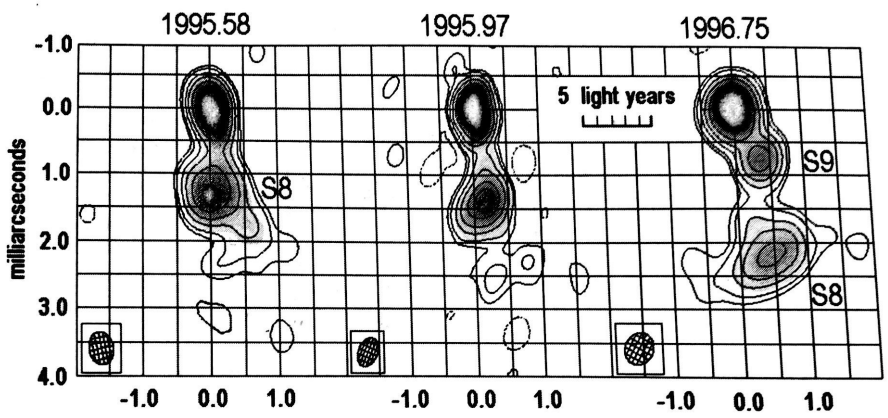

Figure 4.5: Radio maps at 22 GHz of the blazar BL Lac; the scale bar is 5 light-years long, assuming that H0 = 67 km s1 Mpc1 . Blob S8 moves in a corkscrew path away from the core at apparent speed 3c. The hatched ellipse shows the telescope beam; a point like source would appear with roughly this size and shape – G. Denn.

have seen in the introduction, variable sources, changing their luminosity more or less rapidly, creating series of blobs, some times being from 10-15 pc. Brightness peaks coincides with the appearance of new blobs which travel very fast in the jet path before fading in the universe. Figure 4.5 coming from Linda S.Sparke and John S.Gallagher [22] (2000) shows how a Blazar blob can seem to be traveling at 3c.

To understand that we consider an observer looking to a blob created by the jet material, going at a speed V. The jet makes an angle θ with the line of sight. The blob passes point S at $t = 0$ and point T at time Δt later. radiation emitted at T is sent later than radiation at S but because of T being closer, the two emission are received faster then Δt. then Δt_{obs} becomes:

$$\Delta t_{obs} = \Delta t(1 - V\cos\theta/c) \tag{4.1}$$

For the observer, it can be seen in figure 4.6 that the lobe travelled a distance of $V\Delta t\sin\theta$ in the sky, which gives an apparent speed of:

$$V_{obs} = \frac{V\Delta t\sin\theta}{1 - V\cos\theta/c} \tag{4.2}$$

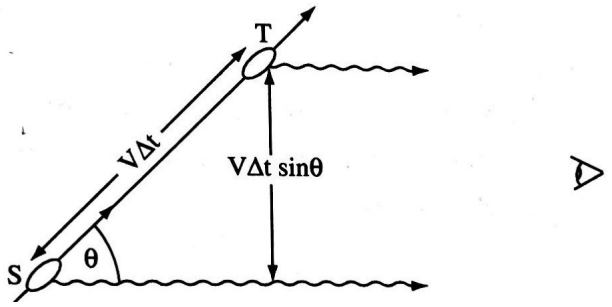

Figure 4.6: Luminous blobs ejected at angle to the line of sight can appear to move superluminally across the sky if their speed V c.

We would only observe superluminal motion for jets that point towards our direction within 10 deg, but this angle depends on the speed of the jet, see Galaxies in the Universe by Linda S.Sparke and John S.Gallagher [22] (2000) for more details. This means that most of the objects must be BL objects as the jet comes towards us.
Blazar spectra look very different then SSDSS J022723.99-010623.4 spectra. It has been observed in radio bands to see if we detected the radio emission of jets, but the FIRST survey image shows no radio sources at that position. All this drives out the possibility of it being a blazar. In order to get more information about this object, we sent an email to Dr.David Hobbs and Dr.Lennart Lindegren, both involved in the Gaia mission in Lund. They said that there is nothing in the DR2 data to suggest that the measured proper motion is seriously wrong, but the high excess noise shows that the source is not point like, or that its motion over the few years did not fit the standard model for a star (or quasar) very well. There could be many reasons for this, but the available data give no real clue as to the explanation (Dr.Lennart Lindegren).
Different objects have been found to be superluminal object such as Quasar 3C 273 (D.Falla and .Floyd 2001 [3]) or the microquasar situated GRS1915+105 in our galaxy (R. P. Fender et alt, 1998 [4]).

Spectral observation of all the other high proper motion sources in Table 4.1 reveals that they all are quasars (spectra can be found in the Appendix). all these objects have error between 3 and 4 σ and maybe extending the maximum σ could be considered.
In conclusion, over 3517 usable sources, 3505 were found to be zero proper

motion Quasars, 9 to have error between 3 and 4 σ also being Quasars, one non zero proper motion star, and one non zero proper motion Quasar which is mysterious. Which means that after removing the biased quasar and the star, we have 0.28% of non zero proper motion quasars in our catalog. It is clear that using zero proper motion to select quasar candidates would not affect the quasar population, the interest now is to see if this zero proper motion correction would clean the stellar contamination of our data..

4.2 Selection plots

The second objective of this thesis is to try to use proper motion to reduce stellar contamination in quasar selection candidates. Being able to use proper motion as a selection criteria would be a major improvement to quasar observation. Even if it is not simple to measure proper motion (only 2 European mission Hipparcos and Gaia measures proper motion), the use of proper motion gives loads of advantages, especially because it is not reliable on absorption features and thus is an unbiased selection.
The first thing I did is to try to compare all our Gaia sources within strip 82 (751459 objects) with the known quasar catalog. Figure 4.7 represents two color diagrams, both in J-Ks to g-r magnitudes, with the only difference being that zero proper motion simplification as been made on the right hand side diagram. It is very clear that two distinct population are formed. The black dots represent Gaia sources and the yellow dots represent quasars from our quasar catalog, we can see that they remain in one of the two population, it is possible to imagine that this population could be mainly composed of quasars.
I have drawn an arbitrary line to try to separate the two population. If we compare the right and left diagrams it is clearly seen that the upper population is significantly reduced by the proper motion correction when the quasar population didn't really change.

Similar process has been made in other bands, such as the J-Ks to W1-W1 band, in mid infrared. The plot of these bands can be seen in Figure 4.8. In the same way as with g-r, W1-W2 color diagram shows two distinct population, with again the quasar catalog being almost fully located in one population. Again we can suppose that the population were the quasar catalog belongs could be mostly populated by quasars. This time the yellow dots represent known stars with zero proper motion in the Gaia data, when

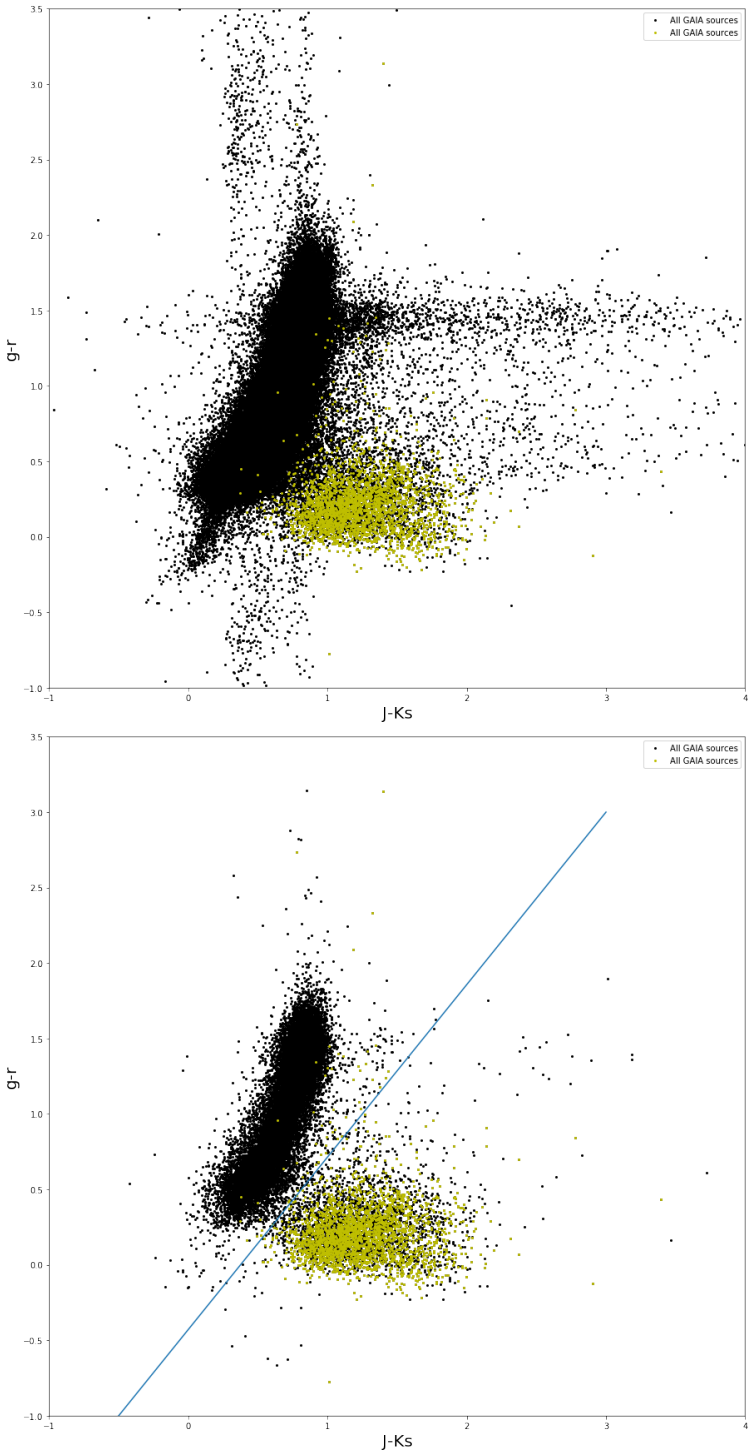

Figure 4.7: Color diagram for J-Ks to G-R band,on the left no proper motion correction was made, on the right the proper motion as been corrected

quasars are separated by redshifts. I have in the same way as before drawn an arbitrary line that could divide the two population between possible quasars and possible stars.

Last color diagram comparison is with the J-Ks to U-G bands. The color diagram can be seen in 4.9. This color selection offers a more efficient separation of population, other color diagrams have been made but they all presented less efficient discrimination.

These three selection gives us a number of possible quasar candidates regarding the bands used. These result will be discussed in next section.

4.3 How many quasars could we find

In this section I are going to discuss the numbers of potential quasars that could be found using proper motion and color magnitudes regarding our color selections, discussed previously. In the previous section we have derived, from the color diagrams, that one of the two visible populations (the upper for the W1-W1 bands and lower for the others) could be a good candidate for quasar selection, as zero proper motion discrimination apparently does not affect it very significantly. I separated the populations by an arbitrary line and considered one of the populations being a possible stellar population and the other a possible Quasar population.
The main interest would be the stellar population being very bumped by the proper motion cut, when the possible quasar population would not be very affected. We already could have an idea if this result in last section, with only the diagrams, but I am going to estimate to what extent the populations are affected.
In table 4.2, 4.3 and 4.4 can be found the count of the different populations for the G-R, W1-W2 and U-G bands respectively, depending on proper motion, from our Gaia data and our Quasar catalog. First thing that can be seen is of course that our Quasar catalog data is invariant to the proper motion simplification, which makes total sense with section 3.1 results. As said before we are going to look at the proportion of possible stellar and quasar population for each color magnitude.

In Table 4.2 we can see that the Possible Stellar Population(PSP) reduces a factor of 20.3 when applying zero proper motion, when the Possible Quasar Population (PQP) reduces a factor of 1.6. It is clear that the PQP population

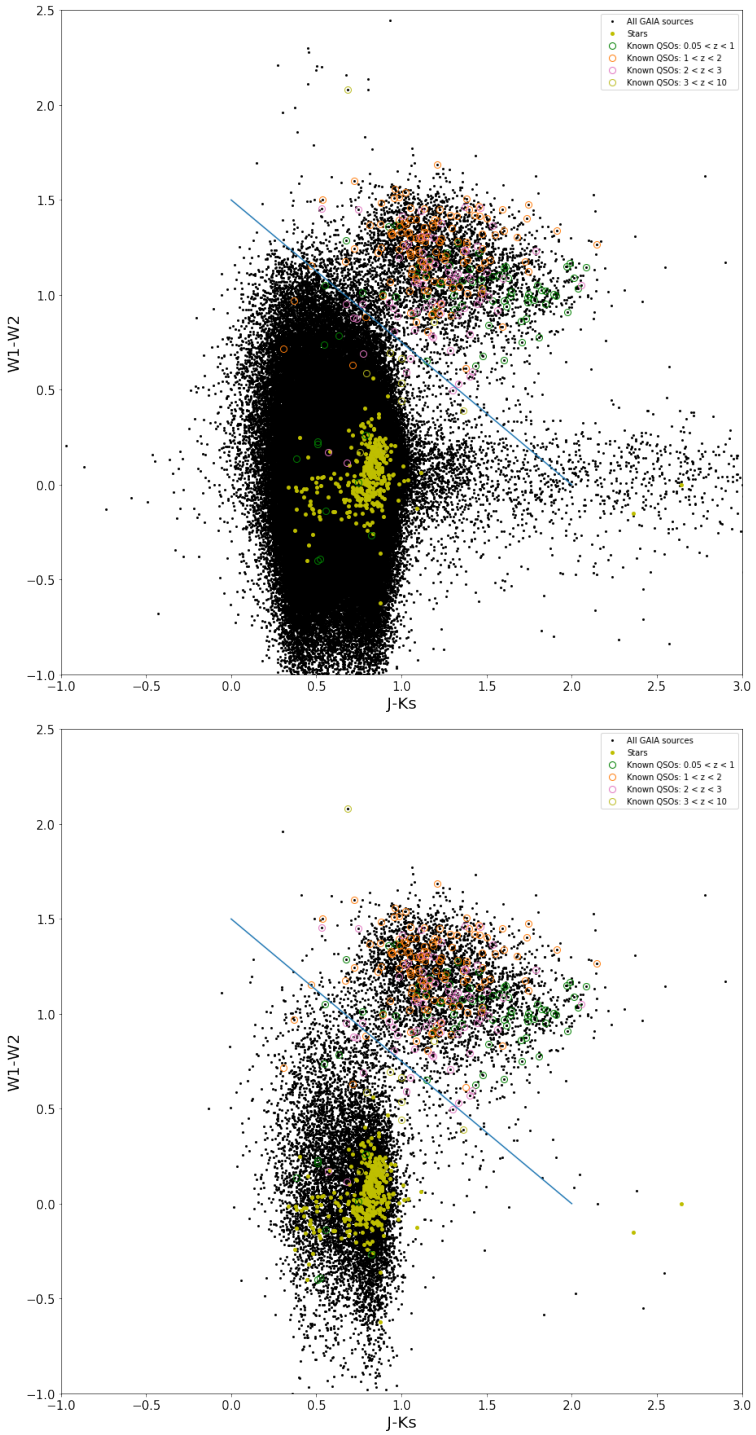

Figure 4.8: Color diagram for J-Ks to W1-W2 band,on the left no proper motion correction was made, on the right the proper motion as been corrected

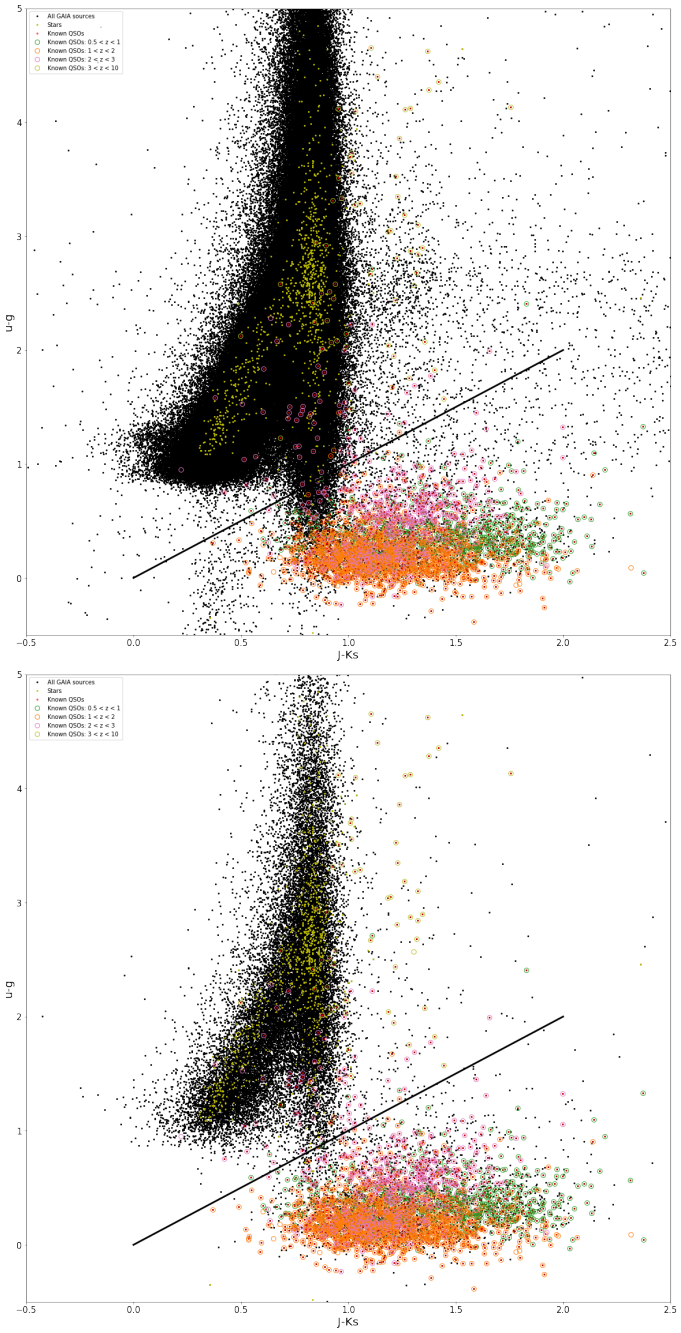

Figure 4.9: Color diagram for J-Ks to U-G band,on the left no proper motion correction was made, on the right the proper motion as been corrected

Table 4.2: G-R band populations

	Possible Quasar population	Possible Stellar population
Gaia sources	7437	547059
Gaia sources with zero PM	4712	26953
Known QSO	2540	57
Known QSO with zero PM	2533	57

Table 4.3: W1-W2 band populations

	Possible Quasar population	Possible Stellar population
Gaia sources	5641	548853
Gaia sources with zero PM	4378	27287
Known QSO	2447	150
Known QSO with zero PM	2447	150

in the G-R band is not very sensitive to the proper motion cut, when the PSP is very much affected. In table 4.3 we have similar results, with a PSP population being 20.1 times greater without the proper motion cut. The PQP this time is even less bumped by the proper motion correction, as the non corrected population is only 1.3 times greater then the corrected one. Finally for the U-G band, results are again similar, the non corrected PSP population is 20.1 times more numerous then the corrected population. The PQP is a factor 1.8 times greater without proper motion correction.
Proportions of populations are detailed in Table 4.5. The PSP is reduced by 95% for every band, which goes in the way of possible use of proper motion as a stellar cleaner for Quasar detection. In the other hand, the PQP has less constant correction proportion, going from around 23% to 45%, this means that the selection of quasar can be more or less efficient regarding the color magnitude that they were selected with. In the three bands that we observed, the color band that is less corrected by the zero proper motion cut is the WISE bands, with only 23.39% of rejected sources.

I used the WISE color magnitude selection to create a quasar candidates catalogue of 1931 sources (after removing the known quasar from the Gaia data). This catalog can be found in Table 6.4 and following in the Appendix.

Table 4.4: U-G band populations

	Possible Quasar population	Possible Stellar population
Gaia sources	8042	546447
Gaia sources with zero PM	4493	27169
Known QSO	2452	136
Known QSO with zero PM	2452	136

Table 4.5: Population proportion

Band	Proportion of corrected PQP	Proportion of corrected PSP
G-R	36.64%	95.07%
W1-W2	23.39%	95.03%
U-G	44.13%	95.03%

Chapter 5

Conclusion

In the first part of the thesis I presented an overall presentation of Quasars, how they were discovered and observed through the sixty past years, with the problems and achievements made during that time, that led to the idea of using proper motion as selection technique for quasar observation. This first part also presented main features of quasars, in order to understand quasars and to realize to what extent their observation is essential to understand galaxy and star formation.
In the second part of the thesis I developed a bit the idea of using zero proper motion as a selection criteria for quasars, and presented the ESA mission GAIA, enabling us to use its very precise astrometric data. Even if the main mission of Gaia is not oriented to quasar selection, its data is so complete, it allows us to observe very interesting things in many areas.
The last part of this thesis is divided in 3 different results. My first interest was to observe if the known quasars of strip 82 verified the zero proper motion selection idea. This turned out to be very effective except for one object (SSDSS J022723.99-010623.4). It is not well understood why this object can have such large proper motion, but as we seen it in section 3.1, some ideas of answer can be emitted. Re-observing this object could bring some answer. Expect for this object, the zero proper motion of all the known quasars in our catalog has been verified.
Then I combined the zero proper motion cut with color magnitudes selection. This allowed us to observe the possible quasar ans stellar populations distinction and correcting proper motion allowed me to very efficiently clean the stellar contamination (especially in the possible stellar population).

In the end, using zero proper motion allowed us to create a large quasar

candidates catalog without excluding any quasars. The catalog will still have stellar contamination, but hopefully this selection technique will turn out to be more efficient than past selections.
The following work to do would be the observation of all our candidates, to see the numbers of quasars among them and derive an efficiency for this identification technique. If the observation of this catalog brings positive results on quasar selection, it could lead to a whole new way of seeing quasars and would simplify its detection. Observing SSDSS J022723.99-010623.4 is also some interesting work to do, as the object isn't really understood and appears for now as a quasar curiosity.

Chapter 6

Appendix

Table 6.1: Detailed coordinates of high PM quasars

Name	RA (Deg)	DEC (Deg)
SDSS J002516.70+002221.9	6.319597862450389	0.37276820174453335
SDSS J010345.56+003746.7	15.939907943508167	0.6296448115955494
SDSS J013306.18-004523.8	23.275753934121894	-0.7566151464446227
SDSS J013446.47-004652.0	23.69363431862323	-0.7811337049212911
SDSS J014243.53-002754.1	25.681390532041892	-0.4650584627909053
SDSS J022349.72-011347.4	35.95720280083486	-1.2298550399823516
SDSS J022723.99-010623.4	36.850034928819255	-1.1065687711985224
SDSS J023617.50+002557.6	39.07294972343808	0.432673149404965
SDSS J025247.33+005135.1	43.19722648138482	0.8597764962657336
SDSS J030501.15+003702.9	46.25481657852392	0.617492169592441
SDSS J214042.01-004358.7	325.1751000331726	-0.7329877821774328
SDSS J230015.18+010520.0	345.0632523659348	1.0889183810881233

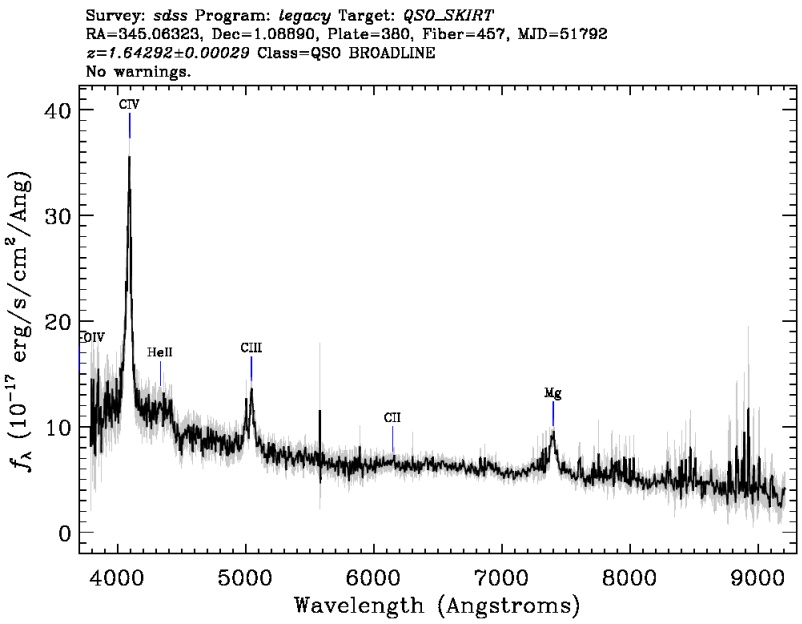

Figure 6.1: SDSS J002516.70+002221.9 spectra

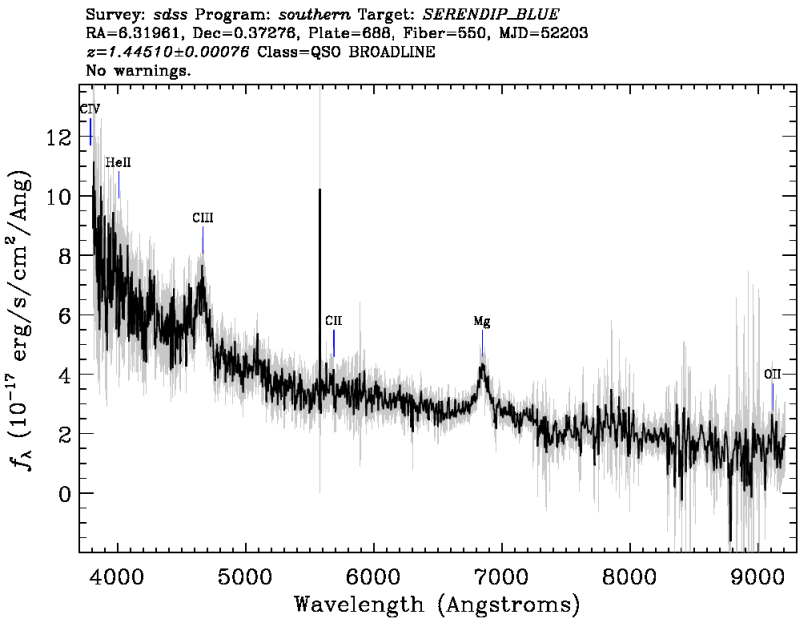

Figure 6.2: SDSS J010345.56+003746.7 spectra

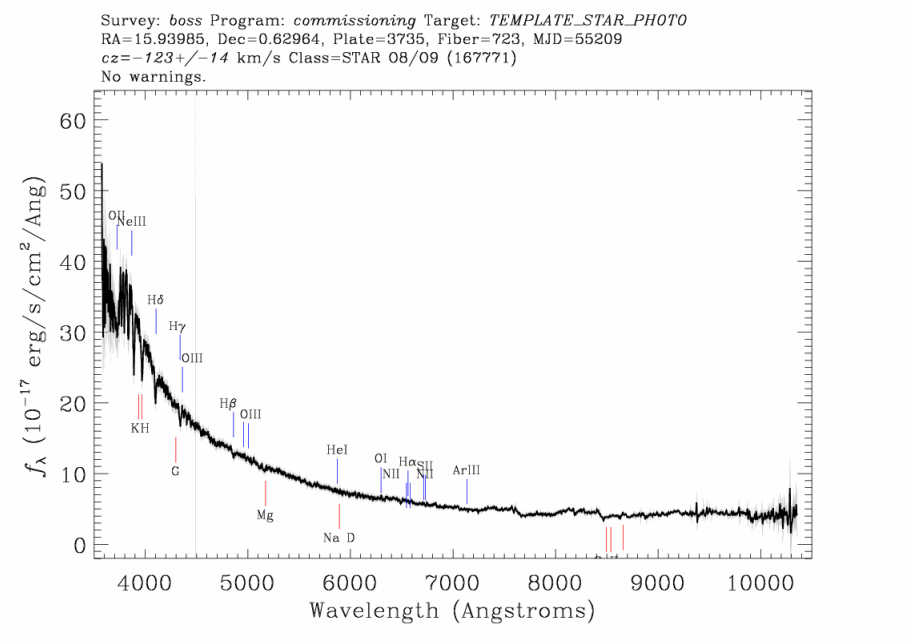

Figure 6.3: SDSS J013306.18-004523.8 spectra

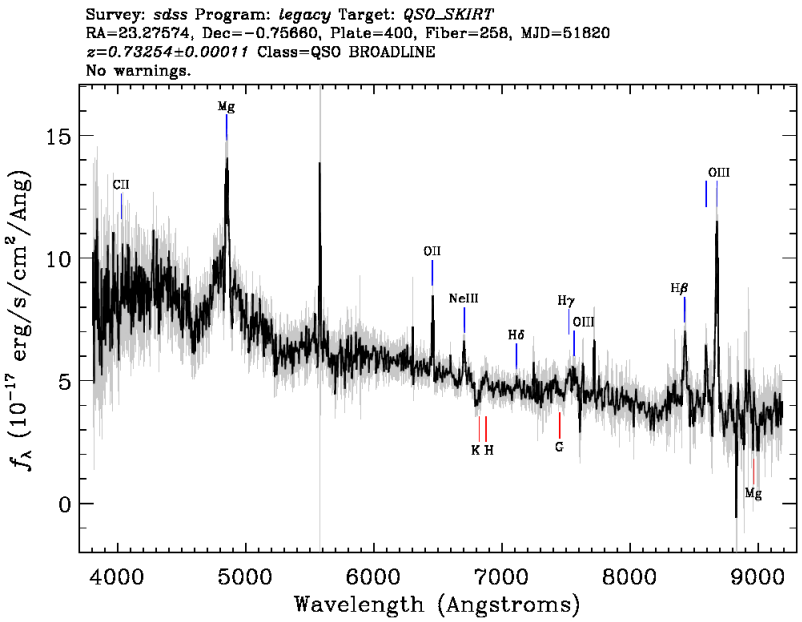

Figure 6.4: SDSS J013446.47-004652.0 spectra

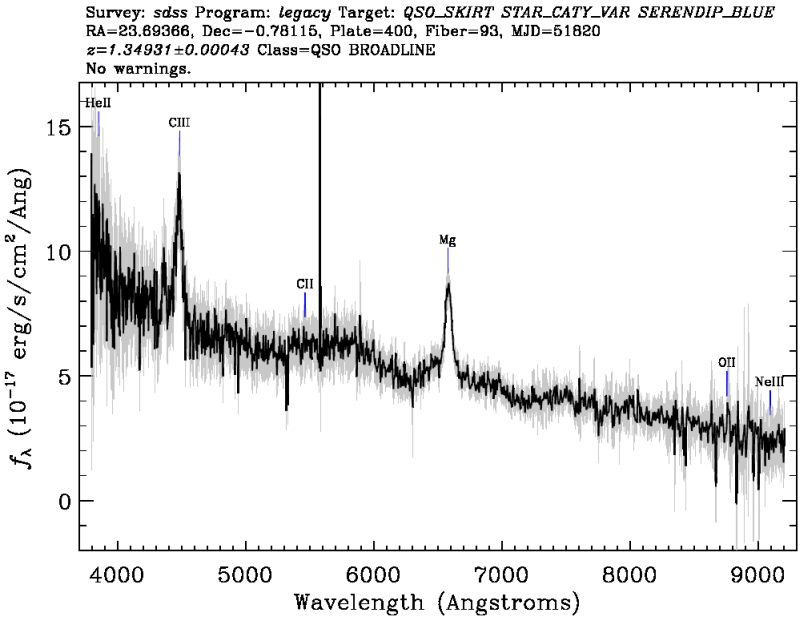

Figure 6.5: SDSS J014243.53-002754.1 spectra

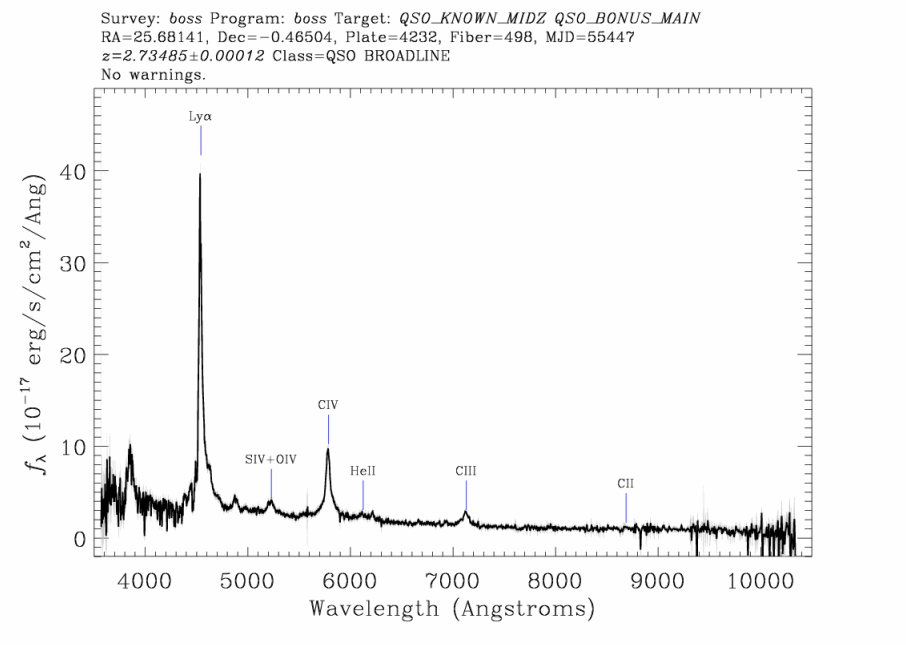

Figure 6.6: SDSS J022349.72-011347.4 spectra

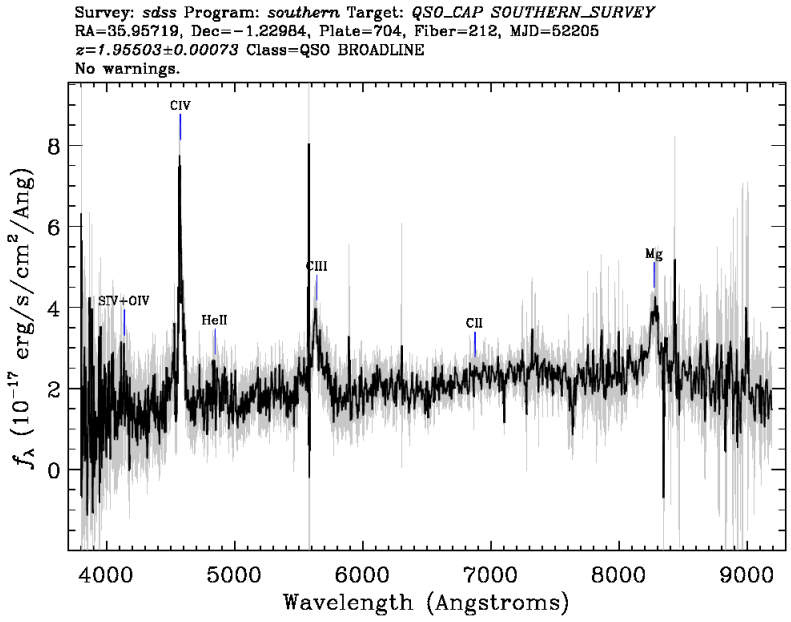

Figure 6.7: SDSS J022723.99-010623.4 spectra

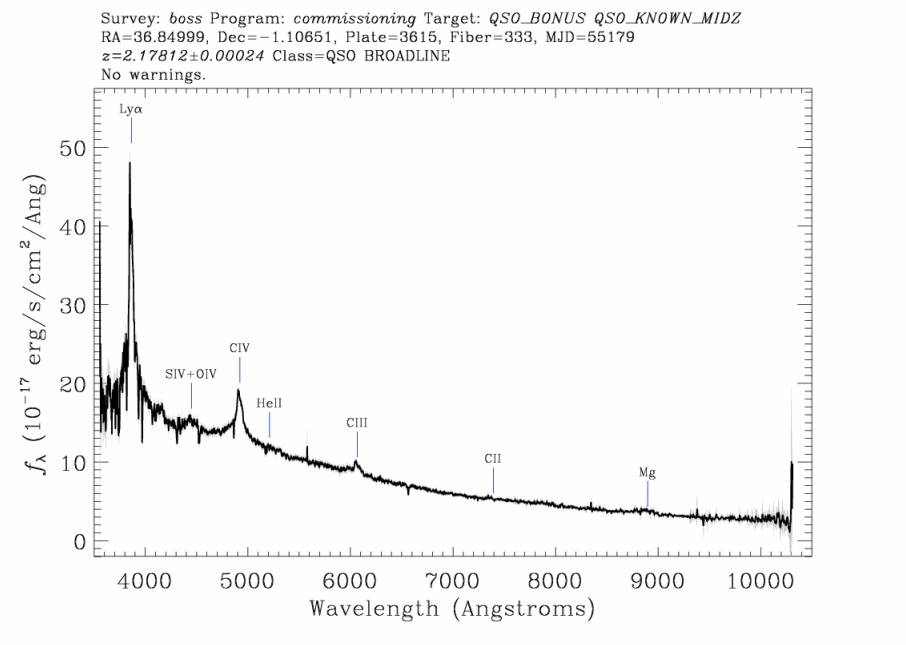

Figure 6.8: SDSS J023617.50+002557.6 spectra

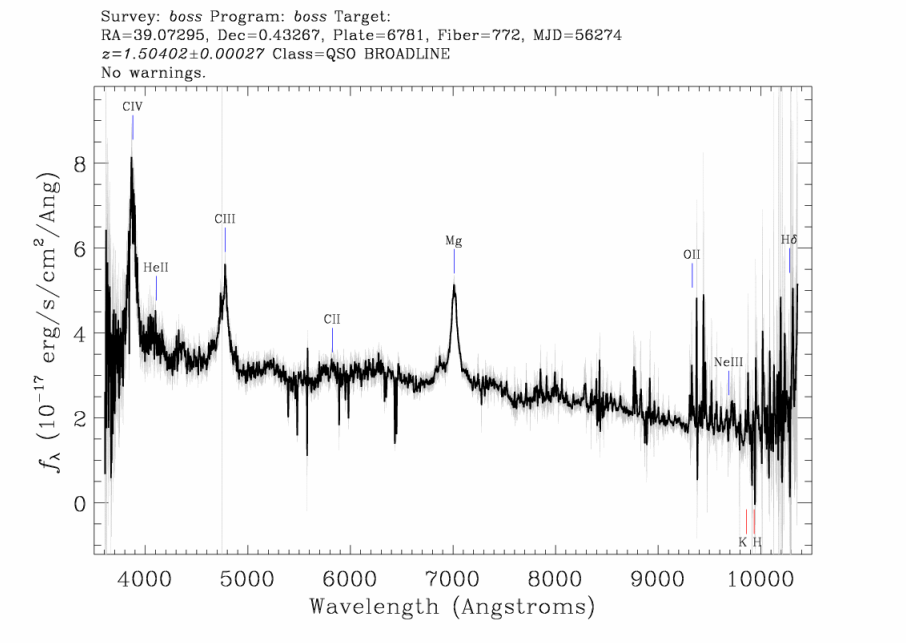

Figure 6.9: SDSS J025247.33+005135.1 spectra

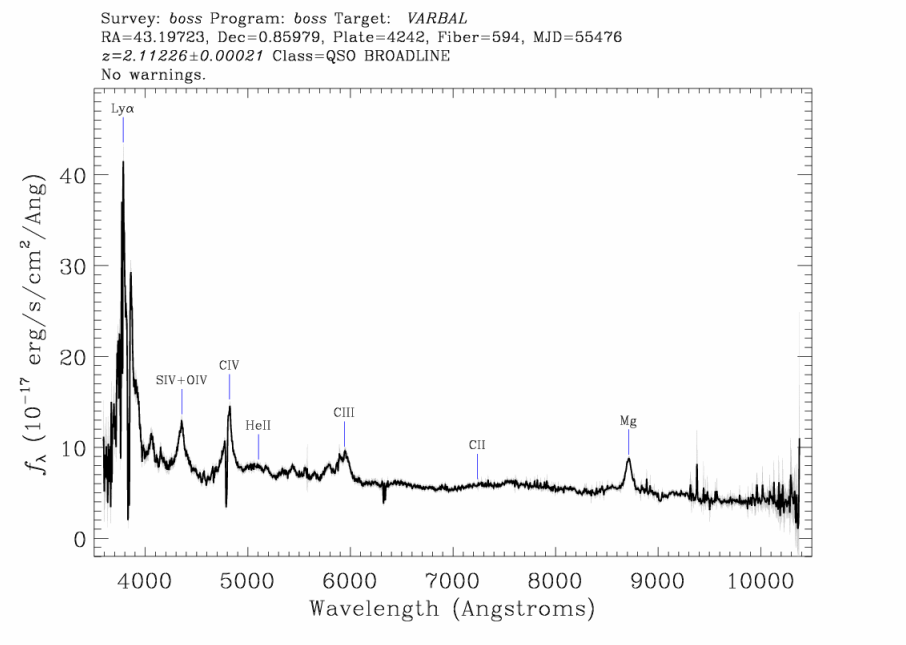

Figure 6.10: 2SDSS J030501.15+003702.9 spectra

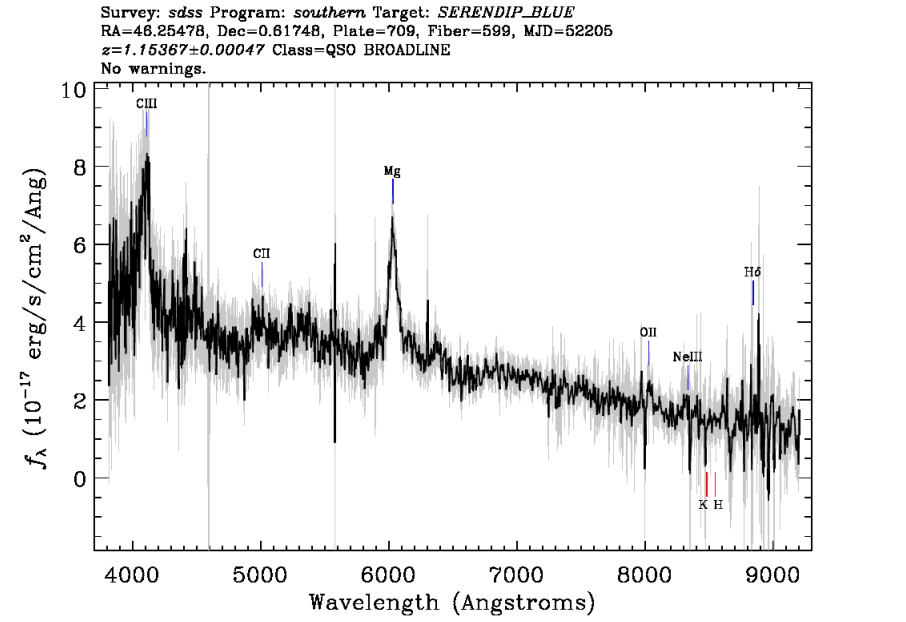

Figure 6.11: SDSS J214042.01-004358.7 spactra

Table 6.2: Non PM objects in Quasar catalog

RA	DEC(deg)	PM(deg)	redshift
345.9470	1.1699	Nan	1.132
341.0128	-1.2053	Nan	2.066
340.8830	-0.2091	Nan	2.033
340.0478	-1.2468	Nan	1.451
339.0738	0.0715	Nan	1.9
338.9312	0.3971	Nan	1.097
338.4862	-0.2954	Nan	0.439
337.8432	1.0717	Nan	3.194
336.9358	0.5807	Nan	1.549
336.8862	0.2991	Nan	0.71
336.5121	0.3080	Nan	1.108
334.2868	0.4547	Nan	1.112
333.25688	0.7285	Nan	1.061
333.0319	-1.0263	Nan	1.95
331.9689	-0.2932	Nan	1.632
331.9361	0.4561	Nan	1.819
331.6549	0.3388	Nan	1.892
331.0070	0.6325	Nan	1.091
330.8848	0.7336	Nan	0.369
330.8752	-0.3698	Nan	1.777
330.7913	-0.0547	Nan	1.115
330.2409	-0.4947	Nan	1.23
329.8541	0.3840	Nan	1.459
329.7839	-1.0345	Nan	2.382
329.3917	-0.2065	Nan	0.863
329.0081	0.7777	Nan	1.208
328.9961	-0.4163	Nan	1.321
327.7199	-0.9640	Nan	1.116
320.6791	-0.4481	Nan	1.971
316.1902	-0.7504	Nan	0.918

Table 6.3: Non PM objects in quasar catalog part2

RA(Deg)	DEC(Deg)	PM	redshift
315.5539	-0.3290	Nan	1.46
314.8749	-0.0423	Nan	1.928
314.7791	-0.9639	Nan	0.492
48.1935	-0.8401	Nan	1.587
46.2868	1.0779	Nan	0.611
45.9557	1.2016	Nan	0.664
45.9167	1.0992	Nan	3.45
42.7612	0.1001	Nan	1.441
42.1295	-0.8404	Nan	0.884
41.8481	-0.4268	Nan	1.866
41.2382	-1.1360	Nan	3.997
38.3789	0.2019	Nan	0.606
37.7433	-0.5116	Nan	1.417
37.7413	-0.5040	Nan	0.861
36.1712	0.2633	Nan	1.202
35.2124	0.6245	Nan	1.397
34.3260	-0.9177	Nan	1.635
34.0014	0.9847	Nan	0.251
33.7734	0.4576	Nan	2.7
33.2458	-0.0972	Nan	0.813
31.2809	-1.2041	Nan	1.612
26.8660	-0.3082	Nan	0.989
25.7634	-0.7316	Nan	0.527
24.9939	0.7922	Nan	1.75
21.9567	-1.1531	Nan	1.584
10.1961	-0.2863	Nan	0.557
2.9419	1.1152	Nan	2.7
2.7399	1.1698	Nan	3.085
2.1638	-0.8935	Nan	2.619
2.0512	0.2201	Nan	1.051
1.9690	0.3528	Nan	1.271
1.9359	-0.9142	Nan	1.268
1.9047	0.3342	Nan	1.1
1.7913	0.3150	Nan	1.431
1.6916	-0.8111	Nan	1.998

Table 6.4: Quasar candidates

Gaia ID	RA (deg)	DEC (deg)
3250472653098034560	57.6941707399152	-1.2320904341115047
3265712227856380416	49.66010632126291	-0.6830768540488867
3265719821358084096	49.87845883592802	-0.5866850285857095
3265960717483800576	48.42829477656297	-0.3781565917608347
3265739715646620800	49.5335297233435	-0.42219758738579266
3265818541182078848	49.905430825324004	-0.4447651437501461
2677296932300277120	332.444719066324	-0.5932088311027534
2677081015704786688	332.53371172108143	-0.9964484039191273
2677317891740715392	332.20737288395725	-0.3933199042061348
2677253535951270912	331.9703783026926	-0.9909181479733812
2677294767637460992	332.36120576078036	-0.6508780743279639
2677095652953595904	332.28436531703227	-0.9330323479487622
2677336347215714944	331.68034414773246	-0.5173598672288827
2677285009471669888	332.2805665337742	-0.8461502724505037
2677066691989136896	332.22449946541735	-1.0483933492181254
2677167739684658432	331.25833684366876	-1.1416836632830332
2677066241017501696	332.21651788659756	-1.1010468639660893
2677324798048227712	331.5004745754868	-0.7378898827951431
2677261954087211264	332.13341995749994	-0.8772568309405928
2677059747026928128	332.16749773712957	-1.1552084803453393
2677079091559667200	332.4277011039615	-1.056862945914612
2677324007774220928	331.4323422751363	-0.8109903769289192
2677210414479765504	330.78565230326126	-1.0516174257779822
2677638914776865664	335.4915757041451	-1.058616842082642
2677530131845159552	334.6454071804817	-1.248178709331976
2677377608966294528	331.6356890210641	-0.31226064240683
2677357474160057472	331.956291298105	-0.4703723609044972
2677590639343874816	335.6124708707405	-1.148641410607606
2677530612881498752	334.69760251619425	-1.2124044514638974
2693157834207550720	326.18931518105484	0.15066414364774025
2693155566465283456	326.39463715680233	0.15912953146318645
2693154570032401152	326.20935426544196	0.10970208326199302
2693182916817255808	326.33811170999877	0.4742553281184029
2693224389020829696	325.8226447735868	0.36974118688896485
2693243389956254976	325.8514922853868	0.5841149648234776
2693438003514227328	325.63837084704664	0.7687752817373428
2693294654685724416	326.9315130782759	0.6744933045206168

Table 6.5: Quasar candidates

Gaia ID	RA (deg)	DEC (deg)
2693437247599979392	325.6868842757531	0.7578371931660794
3257684315504789376	57.71819780993358	0.5137045503415988
2693236346209878144	325.9916275831854	0.5637877579377787
2693211160522253568	326.2794880651659	0.597482449141503
2693232429199667712	326.1412959783052	0.5078195642753882
2693458928595440384	325.44349591293224	0.9577858964374096
2693384780280039552	326.48844418522685	1.193009404738719
2693451442467542528	325.69053862477887	1.0137061660325475
2693453808994394240	325.36834579482786	0.8827656515104625
2693333343751233536	327.227644060721	1.018675477894906
3257754031413671808	57.314216761858304	0.7683315338893448
3257725895085335552	57.20599635963908	0.4301322289268407
3257402084613618304	58.258214722407416	-0.08894420019938284
3257646455369577216	56.87046754916847	0.4124274183247005
3257382190325003520	58.59459655911733	-0.2521126144621037
3257681399224202240	57.742199637307685	0.5198269655674601
3257493584597221504	58.17547375739622	0.2187013493658977
3257532204942678272	56.671894756516494	-0.33249379172534316
3257400366626638848	58.27020201859352	-0.17521268203817136
3257517842572032000	56.93919015216644	-0.3624933122906807
3257671121365199104	57.62495003286072	0.2899224234084556
3257769321497699200	57.909622486900844	0.9556387225199278
3257620475110866816	56.901211161216246	0.12502475274248095
3257485441339244544	58.5185738546012	0.25338411315578957
3257705515463383296	57.83991822628168	0.5724182352912162
3257404661595255552	58.702389198628566	-0.25854576408292596
3257474514942446208	57.97601082262727	0.25711719049192244
3257678444286724992	57.59815653029589	0.37132252137787497
3257659958747482624	57.82500859938869	0.21560888133532896
3257654353812860288	57.70899889857701	0.16014269166573464
3257573711506935936	57.40577895312652	0.09995061984593258
3257514853274771584	56.90610052844052	-0.4785305245547138
3257682395656630784	57.60772271131951	0.45324359694868727
3257667964566506240	57.81756926860657	0.4028034074646193
3257385523219642624	58.57569126656362	-0.2157660492241758
3257415244393468160	58.89189299566013	-0.021297561769269186
3257660199265688832	57.888312709310966	0.23015707336244792

Table 6.6: Quasar candidates

Gaia ID	RA (deg)	DEC (deg)
3257554027673469952	57.492874945110586	-0.12006386994869471
3257582301441273088	56.58744064787039	-0.17673671979896632
3257534099025192320	56.787040481232545	-0.29006099837558974
3257588657992935296	56.62110736342301	-0.048895262713073075
3257650956496054656	57.647256699619994	0.030701426564987363
3257451665716142464	58.231564905296	-0.01730773109648775
3257547598105514368	57.38442785596273	-0.1929941151856579
3257627484497584896	57.251990922087884	0.31629772824887337
3257464589274597376	57.86670049841043	0.0706775746818856
3257586081012503808	56.460313623266	-0.15210284484506292
3257520286410416896	57.06443127545228	-0.354175635560295
3257472079697426688	57.917026907790635	0.1755920835414622
3257762758787613184	57.5702534009742	0.8129984637872089
3257442457306153984	58.17225174004116	-0.15394594771641634
2629974265373971456	337.7986511054769	-0.8650823979335404
2629813805395888128	338.23110242199914	-0.7729902752914625
2629788237455372416	338.29528355086313	-1.0489122616487137
2629958902275521664	336.72415350385614	-0.7075628561696251
2629940008714458752	336.92845594381924	-0.9237804639810739
2629747830402624128	338.4953408562994	-1.0001158963043082
2629890045359765504	337.09238882416156	-0.9954315443635053
2629927909792036480	336.7975803671861	-1.1028873461968278
2629749548389545344	338.499275340419	-0.9780562084471268
2629927222597264512	336.8406377860076	-1.1104921287267318
2629888945848129536	337.1316040817629	-1.0242770858065853
2629920801620658560	336.495385695465	-1.0670184591972647
2629804493906783104	337.96731695392873	-0.9811124130243776
2629784633977937152	337.8203321716754	-0.9759377011008882
2629932479637279360	336.7371431174987	-1.0089510751650321
2677783225678045568	333.93140324198873	-1.014685788699409
2677757563248325248	333.7804409865978	-1.1519946403306858
2677859469936829440	335.2553498725604	-0.6206476295052059
2677793190001794944	334.22634786379564	-0.8143467942907185
2677787937257030144	334.1405303103531	-0.914343919910592
2677938291177402624	334.65621665518415	-0.2921491300288876
2677834627846100352	334.43252042095344	-0.9168430347733549
2677785665219494912	333.99231610358953	-0.9226859476560131

Table 6.7: Quasar candidates

Gaia ID	RA (deg)	DEC (deg)
2677853834940369664	334.94909354953415	-0.6969626068513757
2677830916994350848	334.47656763954905	-0.9866343958436301
2677977461278522496	335.8799841840243	-0.8556801511721186
2677863730544406784	335.26158415322686	-0.5123559742802237
2677901182659377664	334.19364983983206	-0.6549317571595392
2677825144558770432	334.9470103646349	-0.8590431560350408
2677843595738309888	334.6316172814204	-0.7635993285016227
2677956020802150400	336.19552583339737	-1.046005429460037
2677994847306622208	336.47384588374376	-0.7152814563462047
2677885377179695616	334.46268763539666	-0.7679438587728219
2630048134516113536	337.3494731990049	-0.5177081813669623
2629998798227310208	337.8463573616325	-0.7602520765377649
2630085964588096256	337.25697129319764	-0.38707021512846496
2630023399799986816	337.82645566237295	-0.5559482670058011
2630013023159007616	338.0853276940435	-0.505039987571174
2630050814575650176	336.921671152123	-0.6677627188949888
2630025736262202496	337.942433903423	-0.46264327374015346
2630067998740407552	337.55253834172385	-0.5002790656674634
2678328102408940288	334.75783968296764	0.007218729131224712
2678228871484862208	336.92357634759327	0.4773851024005339
2678332294297068160	335.00546853227894	0.06367510648657322
2678254160251546880	335.2106414552203	-0.30770036403183715
2678265086648473856	335.49086475205877	-0.09796911299049992
2678346794106765184	335.4040189159966	0.19558084101661966
2678091569970284672	336.0973342278811	-0.11898181863898909
2678341232124018048	335.374452748166	0.07497057930231311
2678320989943140992	335.23933979662644	0.058307874763812294
2678196264092996992	336.27881675003846	0.14626904396092563
2678071091565479552	336.3091740794492	-0.2720843695979742
2678057313310646528	335.77941559552926	-0.3551517392280297
2678076967080987776	335.92552884782157	-0.3774807227001092
2678128476624084480	336.83565786020773	-0.033119118816457495
2678026801862842112	335.7954157114226	-0.7468018989977859
2678057141511948800	335.77587356146614	-0.37953004203035723
2678096242893938560	336.85948456306187	-0.4821519762876065
2678351020354611584	335.6443757213954	0.2361715898921401
2678054770689978368	335.7143344937671	-0.4528558462623769

Table 6.8: Quasar candidates

Gaia ID	RA (deg)	DEC (deg)
2678085316497888256	336.10421168519576	-0.24992679052664774
2678166302400572032	336.521640515116	-0.20859377274975152
2678306112176005376	335.0096238630345	-0.21569824772415674
2678241756385967744	335.4496993405824	-0.36828735922813594
2678327041552029952	334.7493925100796	-0.047730198618795176
2678254503848918656	335.29044872171386	-0.32970771367612217
2693505657839623040	325.1660357697301	0.9622547954754649
3269786365113678976	56.82031952880941	1.0484049642944882
3269640473664663936	56.302588039377056	0.37939718204280004
3269666140389242880	56.42731656881228	0.46652962011869953
3269740254345037952	56.1069655480709	0.9146564078952042
3269631437053119616	56.082631452197454	0.2140912455394997
3269740597942424448	56.1399798036354	0.9234354564785893
3269711220365698048	55.86050035512852	0.6542413570720276
3269791278556062464	57.28296106220079	1.0249662978718646
3269736028097243008	56.416594713923736	0.9965978990247876
3269730702337765504	56.536066701771844	0.8897416359498836
3269719397983766528	56.24419257203247	0.6645977896566065
3269776194631072128	56.719231178184216	0.8486330522936363
3269760457870894080	56.826708534385965	0.7850536203498905
3269649613354958080	56.55543009542598	0.3430047931359697
3269615184897192064	56.255689171432046	0.11082227099224826
3269757163633037056	57.061355785319485	0.7453617064687552
3269697510830066688	56.014507547586675	0.5741595920545592
3269754311774765824	56.97316602349535	0.640345966204096
3269650201766843264	56.62090920378158	0.3937846978255458
3269616387487922944	56.36833279940586	0.1475418003124643
3269748431962813312	56.38448007228893	1.0594046297034871
2678498389272140416	335.923593687157	0.7754237425485851
2678369643332889856	335.4316533152166	0.4156211194449788
2678610509393753600	332.75050469066997	-0.5806747214687417
2678482583792898176	336.10941334007845	0.7143047339069568
2678386032927925760	336.2727055701247	0.28235491177851363
2678472516389107584	335.77949161101446	0.6522152729197821
2678483752024016768	336.2108630034661	0.7406842431247744
2678394382343860224	335.91337456178024	0.23145779851510948
2678378989181540224	336.1843260083602	0.1646483695199019

Table 6.9: Quasar candidates

Gaia ID	RA (deg)	DEC (deg)
2678492376318419584	336.4194220257778	0.8904451041788942
2530712279763333376	11.83025931556429	-1.02832687017136
2678671497929119232	334.08441668499586	-0.27566305996832013
2678812544655286272	332.6314753063614	-0.2543337287969856
2678896794733816064	332.3043582687427	0.12989183578142796
2678755984230896512	333.7136282603955	0.12364028431030182
2678919742744017920	332.68246579502664	0.3762424034981405
2678917822893573120	332.66169395023155	0.3190796379910367
2678748115850716032	333.5229268774554	0.010837651485586524
2678874289104754944	332.14285851245364	-0.08264234247170095
2678786014642344704	333.73488987187983	0.3333729259075428
2678728599518979840	333.5793556905425	-0.1960942089606852
2678821267733527040	332.2933083397439	-0.2670775193855623
2678851165001080064	332.78476913057347	-0.05069570701186872
2678899333059625728	332.15736554213765	0.14158262214257325
2678664316743803520	333.94074848519006	-0.4015927145414632
2679212900031934592	334.67638879477266	1.0333211275602001
2679136930650219520	334.80054344361486	0.6036063358515631
2678987259629735552	333.78967738964855	0.6106862565642664
2679081302233692288	334.7558816983879	0.1029604437354143
2679196441717224448	334.988451082274	0.9226297280854339
2679028873567981696	332.87386998612607	0.5700861834085242
2679134869065923200	334.99256739773574	0.6192295926900636
2679025987349943296	333.09099254455407	0.7236272297062871
2678997327033296384	333.3623265914231	0.6461150831307375
2679224754140909568	335.36964242190913	0.7488210083455217
6917155262407199744	316.13148253269577	-1.2499136314409935
6917229616881392896	315.89706211945247	-0.785513865034135
6917106196701022976	314.94348483826957	-1.2519345871692762
6917191099615444224	315.51270540832087	-1.1996278248542152
6917233362093970304	315.5762496856914	-0.9007008566628417
6917161722038026240	315.86580113034825	-1.2195920463438987
6917155949602523136	316.19866559095965	-1.1905461605364527
6917241986387243392	315.8218017946711	-0.7309834035585373
6917243154618290560	315.61239307051613	-0.8169679345011887
6917243154618294272	315.60552159095096	-0.8116447585578094
6917237828859995392	315.5164144431667	-0.8119890243714054

Table 6.10: Quasar candidates

Gaia ID	RA (deg)	DEC (deg)
2679364254678685056	334.07656997784727	0.7757751031690316
2679388753172565120	333.98330859093033	1.0241867489884764
2679257602050878976	335.87321265430137	1.0407361513393913
2679303506661773696	335.10245387899226	1.1586867872549174
2679402290909137664	334.34356531492654	1.076761520540457
2679387310063172480	334.01639887499203	0.9498536893562253
6917343519414281600	313.7083069894296	-1.1218423298614808
6917349674102341376	313.910385205997	-1.0341051789866618
6917418183126134144	315.0534460515798	-0.7461736890748784
6917442028784724736	315.2155997075116	-0.6677709639978509
6917413475841862528	314.87696302999086	-0.8044259512628096
6917353758617076224	314.34050043459223	-1.136893443809038
6917305350040737792	314.41981189477576	-1.2081819689925726
6917353999135273600	314.30782481164465	-1.1217956992864215
6917449106891072512	315.09711613344615	-0.5280635941508667
3266218518600967168	49.0350843898857	0.8019758174011876
3266258135379094784	46.14149654336934	-0.9013087546465013
3266160725521307520	49.65955437944216	0.7951587697140312
2680010767516450432	328.17657134297406	-1.088363272068184
2679883842642864256	329.35636633982165	-1.075678916121555
2679985203870603392	328.68849308123464	-1.149698503099247
2680099037684331648	329.06149139103366	-0.6179428062149327
2679882605692289536	329.47266770071786	-1.0670153107425486
2680132023033248512	329.3188561684416	-0.40252778507415304
2680052793771403520	328.0623749020612	-0.8644309642995595
2679897071141629696	329.9563743588013	-1.0128925372237116
2680465037617603584	331.28859850831594	0.28702677064574406
2680247540473592576	330.8506674664801	-0.6522580048643133
2680261250009241856	330.70736509140033	-0.5781749590317977
2680412913894393216	331.3716705373688	0.15901083843383826
2680269771223642752	330.89735873588535	-0.4459526086876123
2680161778566074240	328.7384850330927	-0.5031115004430147
2680216719788154368	330.78595570400427	-0.8762671537819898
2680344400575746560	330.4415432993598	-0.09175329763313035
2680377763881534848	331.039669815761	-0.1377110601322528
2680160713414203776	328.5363049548344	-0.46230979625422114
2680364844619757696	331.02244354594495	-0.3398857753914259

Table 6.11: Quasar candidates

Gaia ID	RA (deg)	DEC (deg)
2680500943543478912	329.8204825192645	-0.27241922685095254
2680682569121112320	330.774290130705	0.5816311511288919
2680484931906216576	331.18863173720143	0.5282916193654273
2680725896750798208	330.21236730957685	0.6784180535170691
2680549871811433344	330.1286838195155	0.13887101582868222
2680735964154626304	330.55559903334176	0.7451080078391144
2530853700151652224	10.55702062281647	-1.0252057456833463
2680476651209222528	330.92191594702416	0.3783127352691683
2680642540025805568	330.66237230152393	0.3360525255610586
2680763623744141824	330.34553659466894	1.0135475001646779
2680541728553167744	330.0724050602191	-0.026117951854349203
2680593233801194752	329.69532236977005	0.07890491564930756
2680660578888522368	330.5056567982346	0.5137446250300305
2680475620417056384	330.99434640875785	0.34878564200925133
2680605809465627776	329.89657612747243	0.29903596127439896
2680508060304788992	329.67253885586877	-0.2521568810843039
2680644154933540480	330.6725681840008	0.4149220933169054
2680495136747609344	329.95893234477273	-0.4202224203707073
2680654875171900672	330.435485251295	0.38690719536525414
2680881722459768448	327.6785474576142	-0.3206662027357277
2680996101733616640	328.1535965859431	0.10178257144428814
2680933876246920832	328.17453741351585	-0.21907666507568313
2680996071668875904	328.20531685891535	0.12300784328817517
2680773111326572800	327.60136071198673	-1.0190892850169684
2680827945174185472	327.85163937546844	-0.5231858971025204
2680843613214212736	327.1660716346835	-0.7619520920674894
2680899482148730880	327.4863877077202	-0.1810930743526457
2680948616574723328	328.6512181206791	-0.17050128816737745
3257896040212344192	58.677263809923936	0.8176647050266693
3258013344359344256	59.59289276461634	1.1683494645061057
3257910643101501568	59.14266119974236	0.8867311015233984
3257870682725342464	58.91021095909287	0.4763856102141075
3258146007309170176	58.15759246252065	1.0230619419434492
3258135531885687040	58.670397491511885	1.2457112952392384
2681225766520324736	328.0644472764358	0.3632449840802367
2681060148285661056	327.21134600545696	-0.36022630652607995
2681202058300743296	327.8614725110599	0.27703820931836903

Table 6.12: Quasar candidates

Gaia ID	RA (deg)	DEC (deg)
2681204154244803328	327.7894051394364	0.32928798786068514
2681062244229464064	327.232026532455	-0.24795671885357076
2681174428775896448	326.7574572884853	0.2787017559306876
2681068394622568576	326.77031637288866	-0.366285206995951
2681214732748238336	327.52266997587884	0.36836147081004317
2681117116732229376	327.18150699620617	0.18181917656157032
2681283314786181504	327.0844982399555	0.6175449214347055
2681369660808982912	329.5016114772215	0.4567321291815063
2681358463829449088	328.9785228336158	0.3738731120474024
2681439789035340032	329.09598180726164	0.737830866661377
2681343822285851776	329.14589220638214	0.23590804815039143
2681326646712355456	327.5616352648863	1.0154124680215326
2681323313817731456	327.5874617236437	0.9728194950009962
2681483563341270784	329.9853449477445	0.8946424078814165
2681483632060923264	330.0144198169035	0.8923113389936984
2681413057158821376	329.0174310117839	0.6284418004511644
2681465661918480384	329.1686556012284	1.0422814714746906
2681502839154883200	329.74730678885635	1.0298720484431734
2681549293521231360	329.4571716812078	1.1279677663906684
2681417214686639488	328.9006573241948	0.663566577418087
2681637293106324224	328.24147907945536	0.9935776381818161
2681673881932223744	328.7225309322829	1.2388011761744984
2681655744285359872	328.7184040972829	1.157867542877886
2681965355592766464	331.4774136706881	0.37225688690429165
2681903542423790464	332.00033170363616	0.20288229956855167
2682094273331341568	332.80225221839027	1.2506123776272897
2681999646612174976	331.8699373344281	0.6621131952662407
2681958689804089472	332.2904148615266	0.7522324218870989
2681962847332453760	332.1886606559979	0.795099102696125
2681935978016898688	332.25828226587834	0.5039943948336053
2681935226397615104	332.13455910593376	0.4975041990384974
2681907425074243584	331.9974910591518	0.28960345656256636
2682092658423622912	332.6144328330726	1.181197311187977
2682000746124013440	331.8324013291629	0.6992536753648597
2681902236753745792	331.8684088322844	0.2720101716858288
3266776486392533632	46.68354632323238	0.9508057625287896
3266853628300380928	48.05935463621202	0.5430750492773657

Table 6.13: Quasar candidates

Gaia ID	RA (deg)	DEC (deg)
3266841254499403264	48.17058802373893	0.5236952293651876
3266854895318989440	48.055715441155655	0.5984574916622771
2682252121969478912	330.82265290096376	1.068245096028638
2682272325495779200	330.8234240011016	1.2591460349464023
2682200891599527808	330.998888178324	0.9838985647554807
2682199517209971712	330.9814711567841	0.9213017470315713
2682225527531694464	331.62421358371483	1.2561263190111258
2682222400796223232	331.737520050846	1.1787059769723802
3269948921035717120	55.70404672188909	1.1248711887499359
3269936040430120832	55.80738941650367	1.0602508655121852
3269930474152476800	55.883560828766875	0.9485837202884474
3269906697213528960	55.82338981290274	0.8908676011172288
3269798429678839680	57.45536283977116	1.0966900194513847
3269812341075933696	56.998530796181015	1.1695630497987732
3269965688588224256	55.19834519576403	0.9599715663187939
3269949612526695296	55.698851830972615	1.1591499963362328
2638800865548760448	349.4156296373311	-0.95540711201732
2638805607192249728	349.74399869705246	-0.8471222291984908
2638786434458592896	349.1813612981511	-1.0873223693706016
2638734413814316288	350.11353116466506	-1.1732757427133007
2638791622779123200	349.0594128339723	-1.0026746234187232
2651768574406438272	345.18829722854105	0.3989871305369828
2652014109096325504	344.21769965356333	0.6682073678623105
2651957106290635648	344.8306578161177	0.4681895448750468
2651871791060231808	343.2354651517686	0.08895011050705379
2651961366898080000	345.06538301458363	0.5220261406552777
2652041356368906752	344.34253341553176	0.8425643522584989
2652022595952036096	344.57764928233814	0.6439369542980932
2651833308153151232	343.8986388261423	-0.032452765644601374
2651888592972461952	343.897945436848	0.2204008517554329
2651809737372621824	343.8770456641761	-0.05379919631204169
2651903509393744768	343.5716708593015	0.26703179756659245
2651823687426612480	344.44559844484917	0.022622652661421726
2652007168429144064	344.0831701574723	0.5854139342752831
2652087364058821888	345.9921087529774	0.46994583827859043
2651932367278976256	344.6943930648532	0.3477252744394716
2651860319202629760	343.62327582569094	0.020612928307432485

Table 6.14: Quasar candidates

Gaia ID	RA (deg)	DEC (deg)
2652023558024388864	344.48702841459425	0.6855044679123883
2651781321868723200	343.69172113157066	-0.46754553594125703
2652054962825344512	344.4362873667962	1.1011924764767644
2651755380266868096	345.27652336977684	0.3234982204119648
2651822587914786560	344.48748515821904	-0.01636853927001679
2651725796531792128	344.82568408255753	-0.019995860592245927
2651748302160854656	345.2034534845954	0.19832807711880268
2652039397864222848	344.692416223119	1.006379465188681
2651806576276475264	343.74644659063523	-0.20112356645950302
2638981838290842368	348.83367664190393	-0.9617005129710765
2639075228059831552	348.78655036084393	-0.5056512238185397
2639082959000843008	348.7533962821532	-0.30868252664127704
2638972045765589632	348.7849519749217	-1.052613389598542
2638957756409472896	347.8637813714727	-0.8653568212459719
2638925801852777728	347.67069937764444	-1.1397504080830296
2638894736353562752	348.3447883531952	-1.0521625375296073
2639038291341117824	349.0350465576071	-0.3693977637704836
2449603192473216896	0.9476970443972186	-1.0503980940736797
2449535950465136512	359.99443703210835	-1.2070515813757485
2449599241103280640	1.0672807193880238	-1.0929692913930016
2652378837718984448	345.5466330209623	1.0211584638150244
2652426975712777728	344.6978637254995	1.0888990157296905
2652128458305543808	345.6206574337801	0.3803153076576623
2652254318027401984	346.8412928425919	1.1883588282608253
2652419141692455936	345.05065486480436	1.1168686265732062
2652167181730852224	345.85335798603234	0.6853220211095578
2652205595918219520	346.66956003861435	0.8434246895040887
2652220714203116416	346.43560808068025	0.8940112389202866
2652228479504068992	346.7056524010621	1.066938541997554
2652286203864532224	346.0951698861677	1.0754530083353975
2652415121603011712	344.7849736993243	1.0531102303815219
2652197555739967232	345.9541120499884	1.1488216325505574
2652422199709281408	345.14246242279955	1.2520840233080883
2652245521934137344	347.1823099200553	1.1859350020541273
5187932640841638016	44.495612957192954	-1.0559855793167578
2652887705444774016	340.8524791120486	-0.891876787416079
2652819329565207040	341.075389060071	-1.2034522683623134

Table 6.15: Quasar candidates

Gaia ID	RA (deg)	DEC (deg)
2652865131096629632	340.6935239109991	-0.964927902934665
2652880455539461632	341.1655360277929	-0.8879777232311513
4226267026359589888	310.2145081631438	-1.0940526568022861
4226321761422983808	310.19038082367655	-0.9744236552555616
4226318531605913088	310.38898238831416	-1.0189434459566569
4226273077968310400	342.16944435121763	-0.5510047510856279
2653233364412902784	340.1448818997842	-1.0211961184342442
2653060019532099200	340.52945244708127	-0.663436812423842
2653096135912526336	341.70540194081434	-0.8317675019753817
2653205051987853440	339.6076195626441	-0.841087282344545
2653014218001631104	340.2595437205796	-0.9913517556093944
2653076787084549760	342.2182027104477	-0.6710495470121283
2653232093102543360	339.6845980585935	-0.616312220228618
2653020471474041984	339.4986018443947	-0.9487108469966383
2653032085065666048	340.0720100938432	-0.8251789162216341
2652950171448685312	339.217480363599	-1.2452038519062003
2652980167500656512	340.2665709012605	-1.2488112667005775
2653069983856274944	340.11729939452715	-0.837646378500003
2653123481969011328	340.32394098137996	-0.6369888559172674
2653046035119097728	339.2706287804448	-1.0385124751594588
2653000096149076224	340.3993760904277	-1.097606577259965
2653045004326942208	339.9615288752381	-1.0642734944413004
2653140799277229440	340.2429578530399	-0.5107560701732019
2653063077548842496	339.8935828765196	-0.8943799609492228
2653117297216032256	340.3038974215021	-0.7853204882056074
2653044115268701824	341.58112304916256	-1.1043369719428382
2653207869486397952	309.22424814987954	-0.8487076388300201
4226511843790151168	309.33520657007824	-0.865578372842372
4226393916873161472	309.3486479527566	-1.1810147702528115
4226393641995196160	309.14927342688395	-1.205132870702086
4226411577778992896	355.08263577647404	-1.0208853932282187
2641051565850681216	355.71641079181063	-0.985658726098648
2640987038261721216	355.0115324902112	-1.1428773051045082
2641065241026583424	355.098624803536	-0.8783692491772858
2641059193712627840	355.0785643583899	-0.8908335311305602
2641044625183443584	355.23768425558467	-1.1742551013670257
2641000060602816256	355.2375667814519	-1.1052239805337856

Table 6.16: Quasar candidates

Gaia ID	RA (deg)	DEC (deg)
4226523350006051200	309.77179614538846	-0.8347192926510307
4226595505457074688	309.47888050592707	-0.4726716998232186
4226575164493552000	309.21944031179424	-0.479260902102351
4226615812064218752	309.163013111887	-0.29775126216758097
2653633311766883072	341.6583218354377	0.3913973675072525
2653322527934117504	341.7548192314588	-0.07625923006900663
2653523120086301952	341.0826009173674	0.0018278359755766209
2653437117661350272	342.3823890389734	0.19983771856160493
2653517588168216704	341.2004107611298	-0.10543565137915513
2653292845414338688	341.8024547559791	-0.41368322442000055
2653329949636750720	342.34954765242634	-0.4238331179241462
2653309643031701760	341.57550624897823	-0.324033440388633
2653311807695223296	341.4195873244345	-0.3122608340805145
2653299438189880064	341.88949157176756	-0.3358686991994581
2653383035433007488	342.4837032696775	0.038378612246174296
2653559232171344512	340.47660351175523	0.017268338154420516
2653339368500414592	342.60039163905634	-0.2686429517917286
2653416952789660032	341.8758167231686	0.0017952826671709398
2653520921063053440	341.24768101587136	0.009298734732521642
2653333046308553472	342.5797932954982	-0.40577683287483374
2653532470229762432	341.3027305358435	0.20032876732883811
2653397810120188544	342.0955500274985	-0.1635805783432721
2653469763707760768	340.981448315612	-0.454053908961916
2653417738768726528	341.76251840880565	0.007360041384853594
2653419800353098752	341.82629568202515	0.07204956853866025
2641264149552091136	354.70826492837006	-0.6414482836861477
2641140007817426432	353.870620783615	-1.1109554588174413
2641209929885115904	353.48231416476887	-0.8461486571655624
2641301945263989248	354.3008957873304	-0.6426358215050381
2641149903421610624	354.0006613327996	-0.9258749617752445
2641284249999087232	354.82446328537634	-0.495431309299313
2641114478531703808	353.69111361726436	-1.245682043119759
2641291843500860544	354.051650272107	-0.7998635775263709
2641131486603798272	354.1485163033222	-1.1260406858720076
2641335583448245120	354.61549175513704	-0.3668059424896282
2641326100160093952	354.3692533535731	-0.5690346980605392
2641175089110290560	353.16360267619416	-1.1238826681791412

Table 6.17: Quasar candidates

Gaia ID	RA (deg)	DEC (deg)
2641279508355173120	354.4846060972933	-0.5530579400943787
1729383081544548352	315.0263675007944	0.060414798183528635
1729450632791049600	315.36646897849425	0.7777328252340957
1729431391336322944	315.49488466542937	0.5991653726347922
1729398543427013248	315.18268775763886	0.3687549447711873
1729440084351001728	315.1276817008545	0.5835127696421979
2653677120433305728	341.31279253110506	0.37476638589287903
2653997628073372288	339.55246570775586	0.1545400762338782
2653901489524834560	339.6347091187202	-0.28489765800698946
2653963199615085696	339.1276207623577	-0.12079413347847356
2653868366737931776	339.0615715024	-0.21166528902991963
2653761576670775168	339.0837776448802	-0.8603391605973756
2653694884418119424	341.13129458680436	0.5405700770823205
2653706016973493760	341.4362294947393	0.7644568404055279
2653835518827104256	338.31255299979523	-0.6540035692283401
2653815693258970240	339.18140072651005	-0.3690313018743085
2653686191404312832	341.54954813892186	0.5424577553949521
2653828372001772928	338.8348152266949	-0.5852145546324097
2653687501369671168	341.6906371897928	0.6081844282003408
2653723471721056256	341.92355107869315	0.9159667807939389
2653838061447775488	338.4997141705512	-0.5543879022013345
2653709109349963008	341.36669220795	0.7996369901294978
2653752643138348800	338.81763983935275	-0.9804662864656275
2653669801809641088	342.2155258964413	0.7363301096222037
2653669256348148352	342.1835726009511	0.7013124631536232
4226870142845526144	312.4484996344526	-1.1084215238937642
4226877775004254720	313.0046878265354	-1.024109976795169
4226882447928756352	312.86461081353224	-0.9687473970291928
4226832454509094272	313.2645005262578	-1.070851217802051
4226862411906364928	312.31145133380204	-1.16336385925132
4226860693919442688	312.42045014511075	-1.172893951924988
4226834752316579328	313.2954399796605	-1.002015335359639
2641567653417319040	358.3251820600325	-1.007265449835491
2641745941803478016	356.03170786021207	-0.9813243864027196
2641865277470200064	357.09749120781476	-0.6133887976983052
2641795149244248960	357.5115887993107	-0.8924909781242145
2641584077372161024	357.8674404264116	-1.1881993960665027

Table 6.18: Quasar candidates

Gaia ID	RA (deg)	DEC (deg)
2641603215746375552	357.4654607591926	-1.0937137481810786
2641753226067978368	356.434572932753	-1.0588190487064955
2641804765675194240	357.046288871047	-0.8725633099229843
2641593865601543552	357.4774884291566	-1.1652401907685304
2641693955519033984	357.08861662098593	-1.1142172267758874
2641851013883472000	357.4546359775709	-0.44377970094741137
2641634036431796224	357.92263200030055	-0.8576932915316963
2641877642680392576	356.5905112421539	-0.5468603496435946
2641850227904866944	357.4823393481823	-0.45283196220522715
2641706599902756480	356.9556291306318	-1.0809032524549875
2641839748184631424	357.3865399340344	-0.6127308212764838
4226908630049197056	312.84365793370006	-0.7053622316855092
4226991913759549696	311.41532494524773	-1.1994935564366513
4227015037862431616	311.12806142548794	-0.9343601645689364
4226957004265328640	312.0520149276064	-1.2172640943764
4227021364350272128	311.40234948427263	-1.02998895762699
4227036925015854208	311.4123425289502	-0.8543462088887885
4227041666662570880	311.4873345461348	-0.888698998080231
4226972466147742208	311.7753166888441	-1.141756573964272
4226907667976504064	312.90658246533303	-0.7168658948148723
4226909381667136256	312.90151064462617	-0.641784128152995
4227011808049027072	311.0678766493159	-1.0368491955436168
1729545396948820736	315.43482295712363	0.8721435680620043
1729606797801633024	315.45746911720016	1.1675718062365277
1729599925853862016	315.2583336113057	1.1052306056242789
2654184270172155008	339.14063328878865	0.35556554798258605
2654031992106676736	338.13159482237677	-0.5025295963568577
2654145134430284544	338.50548583746723	0.31660179044120285
2654296935753731968	338.60044447091695	0.8742094948000937
2654011857299745664	339.4504475244109	0.26667431001432457
2654257731292172160	338.31371109461423	0.5245762060241889
2654086997752789504	338.3704474681633	0.0178763605482227
2654213785187485440	339.3816424498771	0.5319618008944887
1729524265708981760	315.6923188205877	0.6774022154485199
1729554021244182656	315.6380251335578	1.0229410549403408
1729479494971027200	314.6347919831146	0.6500074826270876
1729568555412316800	316.1787890205064	1.1362948095076661

Table 6.19: Quasar candidates

Gaia ID	RA (deg)	DEC (deg)
1729519798944756096	314.86495152907764	1.0344865892708077
1729509353584175872	314.9214852785446	0.9229438092768297
1729544709754083328	315.5996327999578	0.9198138311613072
1729490146490021504	315.11548356081323	0.7024733295016948
1729465235679544192	314.8661140988123	0.6185279223566087
1729543129206079488	315.57732373345726	0.8542444833562424
2642122284017588736	359.3994584490711	-0.025492187725204216
2642037312385006464	358.62647247565917	-0.35390118703261336
2642121012707274496	359.50261889393283	-0.01875388690164513
2642206499736134400	357.90069720298743	-0.520853936954987
2642227772710666496	357.65946480005533	-0.33983233984714906
2642020652207865856	358.0540179128986	-0.49088685382991776
2642082839037769216	359.0934469490211	-0.39883247982349934
2641943991335207040	358.49658044296456	-0.9455977771497438
2641919802079445632	357.09060564108086	-0.20171469142064025
2641947019288559360	358.3392772992668	-0.9020828003261061
2642067480234706048	359.38664112799546	-0.4793122371647758
2641991201616093696	358.81579694709455	-0.47834573268126956
2641970280831570816	359.1206955774069	-0.6005616348757714
2642107303171624704	359.69032377902437	-0.08323097874569385
2642161316680636544	358.79198616988316	0.11721975539337269
2641966050287545856	358.97164548000325	-0.7225557461215941
2642114106399892480	359.7705533141489	-0.008181195577195806
2642246361329237248	358.1005741033873	-0.16416478194793066
2642257562603973376	358.3503418744616	0.06616397248271784
2642136337150457088	358.89662936072614	-0.2545940701206937
2642026596442602752	358.1247197204251	-0.4506848981975273
2642187808039050240	359.43246851928643	0.4089389749451473
2642085725255832960	359.25635207727964	-0.26938722701152557
2642103867197761792	359.6873265699343	-0.12334485594079393
2641975808453287296	359.06829123177977	-0.5494962053197884
2642267114611198080	358.0605952644025	0.12612537187703224
2642104318170606464	359.7285488485942	-0.10214275561031146
2642057142250132224	358.641413745113	-0.19563294217161478
2642249866022586752	358.39356691708923	-0.1191608398867001
2642048273141266432	358.47757434211763	-0.3556862361371768
2642023710224613248	358.36527522699845	-0.4728669005069689

Table 6.20: Quasar candidates

Gaia ID	RA (deg)	DEC (deg)
2641963095350042496	358.9773881079966	-0.7354289758770413
2641974227905313408	359.02170586644866	-0.5800430189671105
4227189654053084416	312.22352278394357	-0.08546972759058451
4227087433830855680	312.5639291339585	-0.7939494352350858
4227096401722718592	312.70628290660665	-0.6335782997640731
4227129799389728128	312.0523182065454	-0.7083937008377039
4227159761081943680	312.2397012351338	-0.4273384268904697
4227146773099810688	311.655678868351	-0.4924407174458357
4227090251329409152	312.4603198695694	-0.7816242848931323
4227097196293101824	312.8524676653734	-0.6244269015049984
4227152476816401664	311.77862313809885	-0.4505836758442767
4227090457487844992	312.44954076289474	-0.774296713532257
4227143680723287936	311.6062866841423	-0.601754782173643
4227095443946457728	312.771349989177	-0.6472938221387698
4227063042711645568	312.40113187821373	-0.8800979220843296
4227079531092409856	312.2676476974973	-0.7642621370721814
3266933652130962944	47.92157179453774	1.0508429139807034
3267154443514465792	46.87433730184623	1.0873448967429888
3267020337455724032	48.34963340794435	1.152997606744258
2654594010051540736	339.66650323252486	0.7524840177453896
2654413243468264704	339.9902878747175	0.8247852965447914
2654401114480509312	339.8504582638368	0.6197926514384454
2654681524305776768	339.2006281033046	1.1900278083592217
2654355832640570240	340.9513129324368	0.5771778005914363
2654498696137403520	341.50066200984594	1.1595967619757848
2654370259436003456	340.5004513335226	0.7098881821587913
2654439356869470464	340.1902438768623	0.95106264568275
2654349403074686592	340.6387333163671	0.45282152292501143
2654472136059756288	340.7353393003445	0.8653263862011089
2654338270519450112	340.448794694057	0.4373856056349947
2654325939668122624	340.4472793931077	0.3818573420567825
2654635482255836672	340.1902918148276	1.1308705855395795
2654336415093559680	340.36769284765455	0.38532268517549806
2654593529015201152	339.71453304967724	0.7396849490862109
2654601672273215360	339.89962217032325	0.8589557360416918
2654644999903831168	339.77631403343344	1.1350560191367318
2654350365147372160	340.5726150945561	0.476071605192654

Table 6.21: Quasar candidates

Gaia ID	RA (deg)	DEC (deg)
2654672625133549824	339.57624916540783	1.1979859272067919
4227261465906205696	313.9595668237519	-0.31245761231700836
4227240437746081408	314.0604401999084	-0.5999237470105477
4227302010398577792	313.5388855560608	-0.4529140973816712
4227342829766293504	314.478376468949	-0.3214008154204344
4227334892666589824	314.44413348615524	-0.4501947904973323
4227318159475731072	313.46958717619	-0.2717568868018623
4227386054317665280	314.44571083926706	-0.07022968350209302
4227428351156210176	313.7837170858951	0.11575439439381441
4227357226496785536	314.07913129197885	-0.2514541094351537
1729717642317588992	314.4372257692423	1.1052387575164793
4227411136926526464	314.13041362603326	-0.13299230704266835
4227488038316653696	312.9853786954447	-0.23465641134685034
4227440720662147200	314.40858004547493	0.16828936006344333
4227492092765848064	312.75371735833704	-0.3354764615676211
4227371421364226176	314.75142340324203	-0.09575950838174234
4227390967760666496	314.396722509118	0.040204543822992614
1729696171776425984	314.2115455123607	1.0481061391034263
1729671737706166784	314.24641531409344	0.8188049166804047
1729667751976485632	314.4245878978521	0.7863231288547184
1729692082967373184	314.277430634136	1.0084783378002526
1729742381328558464	313.96356956583594	1.1377177332461708
2642653623011626240	356.26141117193964	-0.19069798908328214
2642461930031954560	358.75148041800344	0.807013012505732
2642673345501549312	356.9793038526831	-0.05924517359892751
2642665683279806464	356.91440957877575	-0.17164141518752285
2642573324303085568	355.5884635689467	-0.540004381330948
2642601877246028544	355.96546519955126	-0.39552154562584846
2642541266667460224	355.9006666386586	-0.6653950562767449
2642552433582508416	356.1624763431006	-0.4346734164291331
2642440631290195840	357.9596674816737	0.627941708319568
2642439188181183744	357.96350904043965	0.5760749146893643
2642439600498045440	357.9899752225475	0.6029440386297779
2642390667933790720	359.08868759778204	0.4852456744028975
2642596036090492032	355.82230504369517	-0.46144712114135616
2642473857157293568	358.5003881551347	0.9613539804008379
2642483164349686528	358.50172961742345	1.0231910994546447

Table 6.22: Quasar candidates

Gaia ID	RA (deg)	DEC (deg)
2642415789199527424	358.9396446800822	0.8230971028160795
2642559305529750912	355.43965185482307	-0.7779405314128888
2642674616811898368	357.13435276814903	-0.022168041661471228
2642345454814654592	357.8480083614956	0.5212098632520064
2642640153994140544	356.7226689787679	-0.2842149507895216
2558136706805493248	22.053244190522957	0.6293256111554932
2558095754292520448	23.08652578577139	0.6563418952450151
2558092039145449472	23.09984330607908	0.5947866847996915
4227538474117908352	313.3034589673094	0.19411479158461145
4227616024045858176	313.67933786590737	0.12457528195293902
4227615886606899712	313.6526060777869	0.10514435878233176
4227614477857625472	313.63763145080634	0.10057155857582899
4227534316589114752	313.2275201412741	0.014027488942813297
4227602456246175616	312.72772100474714	0.32428662616591164
4227511329923517056	313.3182885025267	-0.1520992520316518
4227566064987372544	312.30516396298526	0.013300995073919578
4227507314130219264	312.8807220907969	-0.06518458730005917
4227539333111242240	313.2147258768703	0.1381940450775603
4227547033987587072	312.647480354535	-0.12810350402091825
4227587337961186176	313.05343203178865	0.19373273028593638
4227560159407885824	312.7053068592199	0.09977154775789275
2643102262411545344	357.714488461332	0.6864589441834272
2642734196598325888	356.51230966506563	0.06134228360401641
2643099925949331200	357.5855160450905	0.6099689130510446
2642747596896427776	356.60233523772763	0.3206005371591831
2642940561186693760	355.676666949394	0.4322380153013299
2643010895571240576	355.3460646705269	0.728545329592994
2643048622564373632	355.8456987265139	1.1248448268059335
2642703444632289280	356.076559941935	-0.1491908511657861
2642830541304721792	355.4325447678104	0.05268268442562059
2642941557619113088	355.63255606894074	0.452600117272013
2643053024906390656	357.33259910407054	0.15817952068487776
2642840196390962688	354.70488937432384	-0.22379335484511934
2643006119567562112	355.416353259192	0.6122983045288306
2643079791142571776	357.2293428684744	0.4275205050880361
2642958050293901824	356.1925394719945	0.5681621002173777
2643078068860032640	357.18754286147094	0.3771761665638553

Table 6.23: Quasar candidates

Gaia ID	RA (deg)	DEC (deg)
2642820920578019840	355.6294215999492	0.10506113048322625
2642881977833177600	355.0705246078153	0.2265532780813094
2643083055317715072	357.1965948819319	0.46091940065337594
2642974955285258112	356.24061379930066	0.7928185674608619
2642906854283862784	354.968696239364	0.4851725272104973
2642908915868172928	355.1085528244208	0.5575111152401695
2643058518168884736	357.2164669389392	0.2734956562204389
2654954516721965824	342.9821534643208	0.5699978312428148
2654989215766497536	343.45528129113643	0.8802832174675707
2654914242813688192	343.4628992958984	0.5029519003386963
2655008324072284800	343.0296620199187	0.9789251755591576
2654980660188080512	343.23983697319807	0.7566725189911632
2654916308692851200	343.6183539580347	0.47696239899771364
2655011863125345536	343.09747152917726	1.1325534157937787
2655036219884468992	343.5183591745504	0.9058208416003443
2654942211640901888	343.48050968490594	0.8628059688499843
2654988288050049152	343.28930674010127	0.8533067217193118
4227731335328437760	313.7883479240303	0.879369328837728
4227661825577408768	314.04922935623466	0.5370816511061252
4227760128789731200	310.6332893514048	-1.0250294232076702
4227652857685648384	314.0353260489369	0.49115309660031464
4227744941786083456	313.4497295144053	0.9979138608162379
4227638220437969280	313.4574946244256	0.3531392919764381
4227676875143017984	313.9753551549224	0.7198530655095762
4227740028343389824	313.4893147227422	0.8922766792466151
4227621040568715264	313.62546235712176	0.23766372856502208
4227756731470552960	310.84654104644153	-1.0644124027610828
4227635128061499776	313.4804683499488	0.3295084540922296
4227660554267176832	314.25376763193526	0.609973946433928
4227744254591258752	313.3763108268972	0.935099330642623
4227693505257155584	313.43272026895636	0.5283897229579585
4227661481980152704	314.2335583671719	0.6432888319937253
4227727006002471808	313.5135874000677	0.8245328368192703
2643381980745931776	356.93182791602004	1.2523286018005308
2643180460880195200	357.08160004833724	0.9559529342888735
2643389265010410112	356.62557676995874	1.1749999061150862
2643404658173094016	356.27630991305494	1.0265478237124435

Table 6.24: Quasar candidates

Gaia ID	RA (deg)	DEC (deg)
2643367927612515840	356.81363621489544	0.9688424543772665
2643419639019053952	355.9933148234769	1.0804537181797178
2643374662121549312	356.77363686282365	1.1084855467869719
2643195961418914944	357.8667129193351	0.7547991955966623
2643211869977772544	357.76834326608883	0.8968642915062929
2643197164009755904	357.76245572296153	0.7822805378080656
2643232451461186944	358.15871587247716	1.0978822888640558
2655101812625097344	343.27650967935153	1.1018880540122318
2655176338897756544	342.1723352840986	0.8907692391157698
2655068277520680704	344.1463389856421	1.1705624080426509
2655169604388722432	342.65290317363883	0.9694813471003111
2655066112857140864	344.03533540677734	1.0993876358253187
2655204037141906688	342.94684306913086	1.1997518205454731
2655105115455163520	343.2196140087835	1.1415486845580889
2655246364044739840	341.84664721553264	1.163671092620785
4227849635907096064	310.268392989356	-0.5113499493597605
4227887843938250240	310.774615997417	-0.19359752947584238
4227805311845175680	311.36543844154414	-0.5434076315008254
4227768409486874752	310.91251925351236	-0.8624625088938539
4227787994538042496	310.81259135518707	-0.6771685564093287
4227857504287223936	310.42720228431176	-0.4414676976202336
4227887191103192832	310.7419568511396	-0.25107215419428974
4227884820281263232	310.63442685486086	-0.21715607043936636
4227888496772084992	310.8883431159858	-0.18452105116650527
4227888496772085632	310.8775344947646	-0.18328117251503892
4227792667461193344	311.19268308544144	-0.7671941391508728
4227762465255095680	310.77185078053174	-0.9544818292508837
4227788716092588032	310.7191956839094	-0.655270863089376
4227840564937968000	310.645637131651	-0.5289319334673935
4227823041470369664	311.21359296154225	-0.36740830909935573
4227895609236958336	311.55603602028407	-0.5208769606704036
4227892688661383168	310.77579733360403	-0.1396283554652099
4227897606398292608	311.57986407707375	-0.45871839758605754
4227942613360175744	312.0651080254443	0.015731124722823675
4227955979298656000	311.64970720294014	0.09934972633107651
4227913407581566976	311.3257814778342	-0.3686728737882702
4228009511771223680	311.6383306646927	0.17278112523779482

Table 6.25: Quasar candidates

Gaia ID	RA (deg)	DEC (deg)
4227953711555651840	311.5644707017069	0.009509197113526185
4228006694272728192	311.4074465972629	0.19434320385090717
2643837797034936192	352.0008255584485	-1.1955202132614826
2643805258362407936	352.83253414349815	-1.1089837114314824
2643875970704001408	352.4155101316072	-0.8218746071874589
2643820204848812800	352.5277319895092	-1.0459313072052205
2644062200486720512	351.58735249332585	-0.8405339280952346
2644209504979967360	353.0156957607232	-0.6912843491163126
2644159060588539392	351.4614076037632	-0.3667685409424252
2644004166888445312	350.9333144197689	-1.010412351132043
2643988876804815360	350.23965791351293	-1.1420405773913136
2644255439654630272	352.7683320387421	-0.71031043894781
2644150676813137792	351.70755837293245	-0.3959009364100898
2643989804517764352	350.3907087954339	-1.1127526855776417
2644277223728815104	352.545566903378	-0.49764776931719773
2644150230136543104	351.81133923621644	-0.38054013370336287
2644081270141895552	352.1022958835803	-0.6162232721174901
2644096285347276928	351.72068291640284	-0.5034909579013677
2644096044829106688	351.6667266031206	-0.5115126488501032
2643999116006921088	350.4738394231897	-0.9658724076347454
2643937302837467136	351.25231044679936	-1.2458493208911685
2644021518556361344	350.765493916324	-0.8801452697398191
2644186105998147456	353.0776267837011	-0.9785095754261176
2644168578236092800	351.4838752933909	-0.22232493813109994
2644024404774389760	350.69146419483184	-0.8519070658452549
2644015368163204096	350.9537478537939	-0.8308554889134351
2644175106586395520	351.48732303150484	-0.08333541131826103
4228057512324526336	309.9970068921236	-0.24671840731467065
4228146783220920064	309.94569401584937	0.13175887615233525
4228127056435720448	309.6223835828384	-0.0023499894743638085
4228041947362762880	309.9673940022023	-0.41308442113713023
4228083969324138112	310.6906315896309	0.06609191502572659
4228104550807885440	310.48921391101527	0.22609644347139904
4228036621603232768	310.1272094350453	-0.5044328597860375
4228058817994459520	309.7741027784609	-0.30618775958597577
4228133928383835136	309.6986764048297	0.09612880748341
4228099706084462592	310.50647557549485	0.1118535956040323

Table 6.26: Quasar candidates

Gaia ID	RA (deg)	DEC (deg)
4228138051552606080	309.6269911792176	0.15143052584087222
4228148015876852608	310.0915624955379	0.19704743475138417
4228058302598385792	309.88503825750485	-0.3051158357055403
4228059127232144384	309.7776086324652	-0.286440718746216
4228142896275541632	310.0756879572204	0.09467653912392412
2644627525556983040	353.8653858774922	-0.22759298037941708
2644332886504875136	351.9914818405948	-0.3496941721546719
2644479465148951424	353.9156954342082	-0.24794914691744827
2644329691049195264	352.87536896267125	0.275463226286115
2644618420226220800	354.0823030829865	-0.014780677166409162
2644366181091489408	352.13921887791525	0.4722670534601892
2644595360547037824	352.0830551627377	0.2389380248389863
2644582269486665088	352.1205012992217	-0.09106782149959687
2644537189509277696	352.2796997709197	0.5712569644831902
2644597834448207360	352.5863302028241	0.2909782556017058
2644450328091275776	352.44357608197316	0.3949732546609818
2644518429092927616	354.1115805945056	0.07917913684452442
2644355701371205888	352.5476170912709	-0.1343434266041583
2644469294666102016	353.74050690601945	-0.300052594066719
2644346527321053440	351.991465082781	-0.14775032963048348
2644528496495425152	354.0646132404173	-0.21878350287882833
2644353674146612608	352.96634286875644	-0.18890576115004892
2644632885676111360	354.08478683184364	0.5495451719276239
2644355185975111296	352.6783303053903	-0.16966124849109598
2644506166961055872	353.2826817768389	-0.027834829416562012
2644667451572979456	353.11756087608643	0.8040716216976309
2644409822254562304	351.7735698914903	0.009123982379528788
2644545538925693568	350.7546248994405	-0.11348472287068595
2644901368376147968	349.5347558700812	-0.2643383057766777
2645130169874525952	350.97933631902805	0.1976803104093236
2644894706882448256	350.0667224628989	-0.25204902011531927
2644758676677637504	349.4275310994883	-0.9636392296649908
2645127455455142272	349.18537698948506	0.0930915704581602
2645042415102114560	349.73860574388823	-0.3539093565697233
2644840177977556864	350.7264216784473	-0.4921923181027085
2644900612461887360	350.0043807690489	-0.306161146066219
2644759840613761792	349.21557817582413	-0.9140333033953105

Table 6.27: Quasar candidates

Gaia ID	RA (deg)	DEC (deg)
2645151575991590016	349.403561463628	0.387460372449838
2645047947020029312	350.6035727531993	-0.23771784557294548
2644953938775917184	353.12248721285283	-0.12217371412188519
2644733078673256960	351.2444165170439	1.0535427542979692
2644922430895878528	350.0865594226271	-0.05082982849833576
2644864431657494144	349.99458862652676	-0.33626358336104073
2644862232634222592	350.0372741069765	-0.4137224840823642
2644770801370328704	350.6007127649054	-0.7714927658223864
2645010804143667584	349.4984825873221	0.37576386991080357
2645050558360192896	348.94530604562465	-0.1259070399948784
2645108557598575104	349.37059258780386	-0.09935754756321252
2645146147152902784	351.35752364888776	0.2841755335889029
2644944180610858112	352.91567687404114	0.1566556400437997
2644736308488625408	350.2963979297952	1.0741872199479778
2645171195402057216	351.20155285513937	0.22914707628745892
2645398656869583872	350.03135295273296	0.6100347624627219
2645240812526994304	351.54511176366225	0.4956494171039504
2645434047400177280	350.8534140965664	0.9217073872533248
2645585475062556928	351.44462510381896	0.7378973683748463
2645429168317331840	350.1790843681294	0.9363170107081958
2645175769542268544	350.5227283614012	0.315815896880558
2645229297719760512	349.8765936717306	0.7641989883899274
2645260530721385216	349.4215988681423	0.7252534303354126
2645157451506864640	351.3163854513464	0.44892991059431103
2645327463491618432	351.2406696358643	0.37478260469969127
2645373024504692736	351.7495321592154	0.3648143586949357
2645424632832419840	351.4805620639644	1.0006939428362303
2645411816649401600	351.7982398986542	0.6861065905127564
2645537710731081472	351.2305393798711	1.2463789122660367
2645325195750878208	351.35637244127	0.29458572686601864
2645319801269933824	351.0726657251553	0.1935912142002878
2645593923262629504	349.80349482544466	0.8556019216861589
2645231874699479680	350.27046395622904	0.34629904622235663
2645280665528645632	350.60660674853915	0.8834369649597038
2645198683192690048	350.16361944975813	0.41403577082771237
2645168584062142976	349.7116460335033	0.21884853854760922
2645236341465486080	348.3243060997829	0.43128775112578

Table 6.28: Quasar candidates

Gaia ID	RA (deg)	DEC (deg)
2657215623729445120	348.9005727124001	0.6219217558971373
2657251667095065216	348.4606669140501	0.8550465161685957
2657175663354157184	349.24436438548713	0.6746622864119068
2657160682508158080	349.09163966230005	0.39263710758703174
2657219300221473408	348.26075291705814	0.6847354356027724
2657231257410719104	348.72348935107	0.6976373502969867
2657185077922476928	348.91034962162354	0.7004405216205428
2657182226064165888	348.82766834854795	0.6047021852033534
2657348389758593152	349.1825129623592	1.153415898239609
2657503184675421568	347.630944621533	1.2497520312592345
2657424397795356928	347.8415794844921	0.8332926674302528
2657459955829276416	348.2034487773555	1.1499664037000963
2657347393326210176	349.3183834614399	1.1988767539262504
2657301351276506752	349.80139010338627	0.9834795942476751
2558259203567821696	22.90209213805457	1.046884159002879
2558205018260451712	23.04348516464964	0.8781936628497118
2645631341017751808	351.49129891944114	1.2336106879800472
2645644878755111936	351.20647422096084	1.1997303892704647
2645601276246961152	350.6616491868036	0.7991577240057446
2645621823370202112	351.25862978231413	1.0279899431803243
2645908113005961088	354.695308591878	0.5375268468268254
2645673603496355456	350.4424476986456	1.1455859223947962
2646033006359360640	355.04130422704026	0.9388663407560573
2645990194125469056	354.27234022015574	0.8341138287459176
2645627046050872448	351.1916029275335	1.1560764180362748
2646016857282205184	355.30330578114626	0.8558641763115491
2645982944220991488	354.5975474613957	0.9262373570322417
2645915186816841088	354.78943174666364	0.6420178379581658
2645957518014185088	353.73338969462344	0.5665667548636817
2645887458507561472	354.17757202301465	0.28150857619844005
2645610209778975744	350.85674119487965	0.9576633944428992
2645674737367749248	350.40764489992773	1.19137873370091
2645632543609034880	351.3305551714034	1.1966218990266888
2646148837332331648	353.73229255510364	0.7223427873821049
2646172953574268928	353.6684218689371	0.9346304873040803
2646054446836014848	355.55348060279744	1.1672023512564689
2646170548392576896	353.4973202051359	0.9156119479246247

Table 6.29: Quasar candidates

Gaia ID	RA (deg)	DEC (deg)
2646195081245163904	354.12967077532585	1.1743037066098572
2646154914711606912	353.6667097877194	0.867162519310055
2646149657670988544	353.7156263824205	0.7275453622495451
2646043520439197824	355.55351433527534	1.0316038749946108
2646428899264694528	355.72327213144223	1.2558846703858355
2646241917864089856	353.1053607725416	1.2453890056435248
3267484193923927808	50.78636173438808	0.9946595136883931
3267679872633354624	50.282844523933214	0.9925795668341856
3267573769761459840	50.935787454017614	0.9524408203630116
3267457736924869248	50.09487355953529	0.6856294917715058
3267666747213589120	49.65611117563453	0.9221550474097445
3267464235210977152	50.15322286113953	0.7586142039415309
3267524807134274944	51.11155700893899	0.8636643582916999
3267715920294646528	49.623360035010236	0.9997973454183491
3267488664984941184	50.55793002261873	0.9203996133745022
3267511922232160256	51.533026894328735	0.8163222034319572
3267458256616466816	50.10411139560084	0.7383414900335638
3267458905155964160	50.30546185217077	0.6527533073272171
3267488866848324224	50.501918428622545	0.937122147570834
3267665201025349632	49.67163271239537	0.8557867955125005
3267674138852757888	49.799441355518034	1.0040310627238953
3267701759787432704	49.95079389307478	1.2076095011775865
3267595622555146624	50.76338321213168	1.2163587909467797
3267590537313814528	50.78790761565749	1.0807226425282486
3267657813681304576	49.95663330080438	0.922390440440151
3267584593079126784	51.28368652174765	1.2037822008563301
3267508005221975552	51.22401293800005	0.7570887053165383
3267700007440098432	50.168364522882435	1.2387805128935423
3267543258313593344	51.54033188699109	1.0462716640288268
3267467117133807744	50.63576060286772	0.6136449552125405
3267542983435683200	51.56372537417317	1.0281427720748986
3267424820295901056	50.96987599938141	0.6879135056439856
3267417402887610240	50.906855297210605	0.5987835935131147
3267410668378884352	51.11411501110229	0.5939352374684349
3267454610188652672	50.08078237481148	0.6007344248822811
3267415027770416256	50.87289465145187	0.5245433348853036
3267489141725764864	50.348675565783346	0.8422916917911365

Table 6.30: Quasar candidates

Gaia ID	RA (deg)	DEC (deg)
3267594213805872768	50.91164895852792	1.215021158956888
3267517076192932608	51.36975601890307	0.9171781100931129
3267482475936969088	50.7942367110876	0.9047994595834224
2674781112257042560	327.32053368738457	-1.055826004967305
2674846743652961920	326.8126570658536	-0.800999773693148
2674851652800021376	327.01126498892086	-0.7317232654221139
2674833235980204544	327.2876675759915	-0.8962020985656953
2702234371414453760	337.2154866064675	0.4945938297246713
2702254471861449728	336.9922133119353	0.6181743906356373
2702252135399204992	336.8893036998504	0.536385606460644
2702319274328021504	337.9756461947065	0.7965533297821192
2702362498879080704	338.55241485393407	1.2356291236456143
2702194033081994240	337.4856041976954	0.5239966324509654
2702381401030324480	338.02052628624483	1.142236420546074
2702394693953926656	337.61628278171474	1.2278587174251907
2702519419804270848	336.4062382624774	1.106574911451644
2702480421500845312	337.2597029215894	1.0699431407902171
2702382393167563904	338.11334765495974	1.185886715043099
2675126702505722368	325.9707844596691	-0.2804013726393827
2675084336948211968	326.03995515168987	-0.5490027014457585
2675005584428352000	326.2190689917339	-0.9442632233478407
2675127011743375616	325.96904611744816	-0.25438402896640067
2675112103912382592	326.41301623408594	-0.4162998389159549
2675085986215581440	325.78050179375913	-0.6944518048223214
2675134570886529920	326.23562870284934	-0.13984202018652425
2675022729937195264	326.03379737768915	-0.843545519906584
2675069562260605312	325.90551426800204	-0.7900297161468764
2675032007067321728	326.1931304716888	-0.6572074504692048
2674963051367345152	325.6138635197437	-1.104751176068129
2675121514185203968	326.0984890865568	-0.3693511732385196
2674963253230847232	325.6025070404098	-1.1019237971536187
2674954903814407296	325.11732406058655	-1.1254440484113455
2674926149008286720	325.8903513732822	-0.9702679411884957
2674921471788300928	326.04428972315486	-1.0204200718127423
2674947104153721856	325.12088406490716	-1.2210708561171624
2674981807489662976	325.35762835718054	-0.9369142851783614
2650045674045072768	343.60932203152794	-1.0784700895006458

Table 6.31: Quasar candidates

Gaia ID	RA (deg)	DEC (deg)
2650006984979878912	343.9256728000854	-1.123435341882063
2650010833270127360	344.2803738788277	-1.0438577109112008
2649996917576064512	344.38942522311675	-1.1589415130688863
2650215651671308544	342.1124352130111	-0.8973772086884306
2650286398372460416	343.1561636257442	-0.5780702171930271
2650219396882808320	342.46677886729276	-0.8543919221499608
2650349143549507968	343.34782301436024	-0.25648076430911054
2650345772000454016	343.32663284396165	-0.2799805645957401
2650247846748953728	343.0441915459223	-0.9231062339051264
2650195860461920384	342.45884458734207	-1.0533586627144664
2650213177770151168	342.35646264835765	-0.8836523859311538
2650287326085405312	343.2960142961315	-0.5578349066758244
2650851551644137088	346.0659130330464	-0.5029306103142858
2650921331977475200	345.8183756209435	-0.20321019509781668
2650627487494646272	346.9375233899677	-0.8563318559668931
2650893569308818688	345.5275684323684	-0.4106940402474997
2650847321101263616	346.19447372287846	-0.5712448367418339
2650754927764738432	344.8702768449744	-0.9563428886266592
2650894840619154176	345.5926584024422	-0.3675097124181764
2650883192667692160	345.34878866160267	-0.6291611334632042
2650870479564468992	345.8454580637762	-0.6725541767953788
2650842618112168576	346.3847224675327	-0.5277010672886066
2650883158307950208	345.34196252650304	-0.6340942329322261
2650706446173774464	345.4527025017778	-1.1696288306147984
2650710023881781248	345.4814694539298	-1.1136225132975606
2650607833724597888	346.26860156093164	-1.0809374568821999
2650785679730230528	345.33529682978536	-0.7282807119435166
2650890923608936448	345.61046922751984	-0.45243548354084023
2650877592030410496	345.7376734421414	-0.5380003784709925
2650994140263279488	347.68037826368254	-0.5308410030870654
2651150958108843776	347.67056269935296	-0.05274673978961884
2651198481922660864	348.01032976436494	0.3250779357171751
2651052139501715456	347.4311329439207	-0.2434644068276638
2651306057967903872	346.0448498704773	-0.0010928951801014858
2651210469176248192	347.9495659950181	0.49500925763768017
2651200367413107968	347.83846044680115	0.3032924030347451
2651081139120277120	348.204290132335	-0.4245341632781005

Table 6.32: Quasar candidates

Gaia ID	RA (deg)	DEC (deg)
2651288912458348800	346.1844412551885	-0.13749346288280093
2651161266030322688	347.5034596300268	-0.0878401885349851
2651068700895309696	347.28146099625513	-0.13191853435197504
2651026202194379904	346.8085640247669	-0.5576267025159389
2651392580084632192	347.78922362304706	0.45795490857832816
2651315369457174144	346.1454135809707	0.14160981593574415
2651396527159148160	347.64635204043185	0.5163275039971532
2651324032406618368	346.53842214917626	0.14559573394085767
2651575507035995520	344.35021772214765	-0.6203337461831501
2651407664009732736	347.5006879211514	0.5355600332256819
2651688069538974592	345.3825296640519	-0.12120534079646962
2651709544375460864	344.95464679501373	-0.11508810484805695
2651630173380272768	344.62760644264614	-0.12068439130497614
2651651854374674560	345.335244116102	-0.21723764029327575
2651643298799749248	345.2403177511801	-0.3507174158865789
2651378728814374272	347.2236474787016	0.38426510420950616
2651443153323860864	346.8173563157099	0.5234391066186234
2651472668339500160	347.4036492237525	0.8709578655800149
2651538020561808512	344.8685225039152	-0.6375744569162681
2688841426435363072	319.0134632901193	-1.1412302800335818
2688908604019436160	318.6269964721861	-0.9467373001823641
2688836031956406656	319.1585414944565	-1.2417637197754092
2688842147989881088	319.0468177566826	-1.0787399628028131
2688918362185230336	318.2039038241693	-0.926901486339721
2688848538901679104	318.59749894506234	-1.1863884828812123
2688837543784917632	319.13247467488236	-1.1798569022060068
2688858262706994560	318.8422474296549	-1.0031477816773922
2485832581644635008	21.697527588148137	-0.8810122916478998
2485886977405749376	22.73527637398843	-0.7667191887325393
3251035809209843456	54.82982997434607	-1.2226932797721142
3251222313869274112	57.42978970981389	-1.243206884042807
3251231556639215488	57.130817632296946	-1.2179727523485409
3251269558509852416	56.3185656546503	-1.2104488816230268
2533672332569284480	19.14167216572078	-0.9517186380467167
2533608668269342848	19.550142290745068	-1.078496236897052
2533865301155105152	21.039157540842563	-0.8328163305550382
2533656939406067968	18.71127662974428	-1.0214129928442341

Table 6.33: Quasar candidates

Gaia ID	RA (deg)	DEC (deg)
2688997488366836224	317.4263319848758	-1.015911886556834
2689027243901046144	316.7705701135687	-1.1789002169423315
2689075248750252160	317.9033399888523	-1.0063057282174754
2688998106842114944	317.3821531952435	-1.02994716973253
2689045969957697280	317.2231521428318	-0.9877602527989284
2689083804325201024	318.0246436431566	-0.868424429761979
2689063390345187968	317.16554330018886	-0.8046865241667903
2689057278607208832	316.95066628999353	-0.886454769112414
2688927325780938752	318.4168736852219	-0.7391743412667641
3263550484916674176	54.574417478842236	-0.2530794577626511
3263644183923239040	55.413307397090655	-0.0035269782022932703
3263563369818375680	55.55190956739196	-0.4917408605019895
3263530728067390592	54.941085184838684	-0.3838341815840232
3263479295835161728	54.910848079070554	-0.6071329414298299
3263744102042335104	54.4069516997658	-0.07703350364027765
3263778186902768000	53.74366390362461	-0.12885823913981692
3263496333968912384	54.47623327198011	-0.753922266740886
3263605052477285760	55.90699342946499	-0.06394947128817643
3263764786605032960	54.52815531314811	0.0760861326636838
3263768188219209856	54.57800384575878	0.19822608354204294
3263622124971568512	55.68148635836828	0.05647610275006307
3263732900767605504	54.212846254309696	-0.11605573679030538
3263576873195628288	55.637720696957224	-0.2468036598112787
3263725101106918272	53.924795923314214	-0.2958176382542859
3263755509475458304	54.28522641500277	-0.10401255694936931
3263734206437659648	54.09788538505569	-0.12462799849262848
3263575498806066688	55.69297590450654	-0.3052704910332793
3263533545565936256	54.84859714198338	-0.3861950315789858
3263535126113915136	54.853090323696335	-0.31376265442082496
3263566393475352960	55.43637829583666	-0.4817822583515287
3263798669602510592	53.62267547108224	0.10304643608384326
3263803784908099072	53.6858114822972	0.1050839922421178
3263729636592407936	54.15047236188519	-0.2310018284936078
3263536844100826112	54.97608249776916	-0.3486020969038374
3263580068651247744	55.39756199812653	-0.3760691419904712
3263467299989889280	55.48365843683806	-0.6184304016207789
3263438128572382592	55.031776519614695	-0.7757178446680271

Table 6.34: Quasar candidates

Gaia ID	RA (deg)	DEC (deg)
3263648066573860224	55.43287871302191	0.0654561836703892
3263504859480557568	54.576226693816544	-0.6196389543239899
3263595358734971008	55.610435478337415	-0.0741964053867201
3263484789096734336	55.30195566069673	-0.4978312238148592
3263679024698252544	55.839613014188664	0.2938709877685312
3263750875206508288	54.60932552168417	-0.04834314008164216
3263414626511513472	53.48839847141615	-0.18503478783198798
3263649891934764672	55.011851091362125	-0.1077947950594614
3263498051955837952	54.5027555177398	-0.7128373556106805
3263555093417973888	54.91559794311577	-0.2074656285555824
3263600615774913920	55.945876913833004	-0.1184796548204776
3263757399261094400	54.39121550089563	-0.051296234626809635
3263465723738544384	55.3984898588866	-0.6756340239017837
3263836186141542912	54.16459391230521	0.42649644447862056
3263687648992583424	55.52865006847287	0.29487993772229565
3263411293616542592	53.20163957855307	-0.22092555200578154
3263724345192654848	53.86903935100935	-0.36478611681081313
3263763893251874176	54.31899381632702	0.13420385442476973
3263655213399254016	54.91348664371501	-0.005591296760238475
2689162518190040704	317.3196362257706	-0.6157267186735542
2689145166522059392	317.48764476438856	-0.7490117253329674
2689117644372112000	318.397546620101	-0.6457480371532993
2689107340746299520	318.20414804668616	-0.80656332877384
2689143242376685056	317.46966923758094	-0.7959490745921549
2689235498274428160	318.89364383001185	-0.8730279247430196
2689236288549028608	319.0693650877778	-0.8614859116796028
2689162037155676160	317.4439386312047	-0.6091965994296962
2689127539977436544	318.00408133044596	-0.6097849947249482
2689258828536515584	319.9025583679765	-0.5977242033298471
2689136576588041344	318.2043138196734	-0.4212302342092842
2689136714026995968	318.25613286994906	-0.4174831298791735
2689096994168840576	317.5954676810295	-0.7977045319194561
2689130602289002880	318.0041557403842	-0.5787568144815902
2689111326475999616	318.12453124381216	-0.7709399711456486
2689159425813915392	317.26309841602665	-0.7092496542140414
2689199386194054016	317.588771741509	-0.30887644702408473
2689107920566619520	318.14128630109803	-0.8016843997909716

Table 6.35: Quasar candidates

Gaia ID	RA (deg)	DEC (deg)
2689123799060965376	318.3157664621439	-0.4738352682953582
2689181729579763456	317.7852463647356	-0.46421714000918235
2689154997703167488	317.5704490766319	-0.6300789976686819
2689108199739758976	318.1947141323696	-0.7878130779519217
2689192071861026176	317.8861109280891	-0.23845470852990847
2689119156200630272	318.44403838711725	-0.5716105989091265
2689163171025118848	317.41452870838685	-0.5576424497797783
2689414134554876032	320.1089236619605	0.12640202970608422
2689321088383861888	319.2554524181975	-0.44410426632845224
2689343563947428480	319.0594205467857	-0.17678556081213787
2689331155787103744	319.29361099864144	-0.3219014104931518
2689294631385051392	319.11019910378263	-0.5818726459187052
2689480895526767232	319.722302682103	0.28691625562439793
2689376476280877696	319.6884541551796	-0.25833780081888297
2689374311617360000	319.84529474366815	-0.25938353319475194
2689296658608843136	318.8956548087158	-0.6162973193079325
2689363316501009152	320.1074456514185	-0.33000817065746346
2689317652409771520	319.25172462902816	-0.5649854681067225
2689339127245665664	319.149535086451	-0.26000894922136775
2689365962200852736	320.00613349307804	-0.3431520389041885
2689275664808370048	319.57031240706874	-0.45332562276509014
2689387883713992320	320.2810312292879	-0.2776277721056539
2689377781951005312	319.7680139447811	-0.20801407321677082
2689480277051413120	319.64800132173656	0.23669618930442954
2689392144321829248	320.37558486611846	-0.09085428425212809
2689327238776906752	319.43379529641066	-0.36752130079662865
3256519623453140608	58.38340855436497	-0.7405234782588824
3256466675096567936	58.240663881582044	-1.200799199665662
2689580336904429056	318.2861024216502	0.06166922343029819
3256620061264593280	58.588619516302465	-0.5270278134902638
3256477910731034752	57.71396714825934	-1.170625425814149
2689517660445819648	318.3225634397313	-0.2835329378363991
3256510140165311872	58.335926631833594	-0.8822940593069866
3256449220349144832	58.718262849221475	-1.0466412228872435
3256445475137660032	58.547697963845856	-1.0605059510806047
3256583566926479744	59.149155144727914	-0.5920241325776644
3256522303512742144	58.26326451140403	-0.710800875197521

Table 6.36: Quasar candidates

Gaia ID	RA (deg)	DEC (deg)
3256753926805448064	59.93120429941504	-0.6870652632717977
3256538078928900992	59.170383375664706	-0.947871332325635
3256490692553734144	58.317932110000115	-1.1373419923989136
3256636446563507712	58.96905668567154	-0.4178569157364742
2689598302752745600	318.1274077203587	0.24091356870915018
2689631940936792448	318.5211951847995	0.4593913554511406
2689543464610543616	318.97035129105967	0.020988505261675117
2689561915790169984	318.82704256913263	0.18757012709315019
2689586727815711104	317.9474444552205	0.013909937479302038
2689499621583059840	318.4540618739993	-0.41274409001403495
2689599814581014144	318.55244424139113	0.07650087198596218
2689551474723303808	318.612621186323	-0.007530927271829476
2689657779459044224	318.9550662523518	0.30857930694454816
2689631567274423424	318.46664329784227	0.48576327088093774
2689587655528653312	317.9277170389488	0.047612913546813754
2689649395683325440	319.3068845842124	0.33752704872507494
3262689876550173824	49.90446304243348	-0.9723738810785386
3262664244185310848	49.72812436373402	-1.0724739624085968
3262496332438979072	51.48401233421168	-1.1336247254602108
3262794914269806208	50.323499372338055	-0.6667577862585141
3262764402822391168	51.27321999386584	-0.5793160080036995
3262556148447937408	51.432635629542304	-0.8763155237023552
3262723209791437184	50.495465354694005	-1.0104816351989718
3262754850815294336	51.03991114593986	-0.7882659410773564
3262645861724811776	50.253115214629844	-0.9798897248705972
3262631155757196032	50.07260652523274	-1.2386224681192433
3262714718640560896	49.81491565377816	-0.7213750441029003
3262643800140489216	50.122407306495376	-1.0504064477988124
3262530722241863808	50.81318280925315	-1.142159484475978
3262734063173574784	50.73989925293903	-0.8112269695571617
3262704170201355776	49.69222831259886	-0.9397051973739221
3262804431917381120	50.379498299918545	-0.5095739859669438
3262531649954804480	50.733693675707805	-1.1358357698608743
3262819103525683328	50.2373104652793	-0.4461594002551988
3262696198741550080	50.06443127630024	-0.8715344769482127
3262494575797084800	51.43675881092407	-1.1745927987608136
3262574840145645824	51.37489333155724	-0.6898000319855535

Table 6.37: Quasar candidates

Gaia ID	RA (deg)	DEC (deg)
3262569823623833344	51.331091168536524	-0.7503067846420352
3262644727853437568	50.27732396420836	-1.0110750202833656
3262631263131077760	50.076287106561836	-1.2242182908950687
3262780689338635776	50.95639451612521	-0.49718415232053054
3262732310826905984	50.69508338514846	-0.8636099235260745
3262803435484953984	50.55026855238919	-1.249449350420867
3262622668902175360	50.16991114872444	-1.0243984857181576
3262644143737882240	50.89919255901811	-0.8759483678279203
3262729871285479168	51.37217452322848	-1.0223334871828136
3262545084612152320	50.30470089528542	-0.7624715144176776
3262790928540135808	50.343153021322756	-1.1001171832415013
3262640295447158272	51.00867938501107	-0.5098626380484191
3262779795985187968	51.24001297874835	-1.239602686343948
3262517184504903168	49.77801103821691	-1.157954429114014
3262662388759405056	50.27847981344489	-1.0926851811082872
3262639780051085952	50.325904050674424	-1.0944212960379673
3262639024136841344	51.11990446705736	-0.7705031149212757
3262755164348126976	50.724180192114446	-0.694247889885003
3262747880083569536	49.750562714864856	-0.8530022258374893
3262706609742805248	50.998205461045636	-1.1991076401122156
2509594745908196352	26.43803890878576	0.8142971515924189
2509587702161775488	24.144667961565926	0.6786925653199457
2509640478719305088	23.672907287000207	-0.9662938488759264
2509759054176774144	319.69303639038037	-0.3159883364870458
2689679323014734464	319.6245906180822	0.5136970071805389
2689673138261812864	319.72364765059984	0.47511387753209633
2689678395301784960	319.5424064719549	0.47888316970224964
2689700900931461120	318.9716502963802	0.7543192051125656
2689758762730380928	319.23602084899846	0.8340058112296458
2689767009068288256	316.1072819115536	0.9765988864883983
2689846002105521280	319.578819287737	-0.8221329093956598
2689699354743223552	319.5177939006213	0.7445037022835381
2689701072730156032	316.44894883582344	0.7554142872855014
2689789171099213696	319.09725733199764	-0.9263324127875133
2689761030473762432	316.55310407386446	0.9138477285744238
2689835797264675584	54.662682550231295	-0.503839017219359
3264725622328625920	54.31222616054733	1.0469648802734697

Table 6.38: Quasar candidates

Gaia ID	RA (deg)	DEC (deg)
3264703425937475584	52.6133737320536	0.9661808153887899
3264849592264745216	53.075163522587296	0.9093882983831646
3264871307619164288	53.061670801091864	1.1134738285182684
3264868524480341632	54.02444099589332	1.036252687886128
3264719437575799808	53.125210238663556	1.028959492220978
3264878145207138944	53.42087737124373	1.204590547419985
3264687246796285440	54.226029467708535	1.147926391592527
3264688238933063168	20.386808326757954	0.6711223737986707
2534226520789377280	20.212249675978654	0.1079834967013
2534138972175657088	21.190452337064745	-0.309168003700021
2534317161778870784	20.64642121022577	0.5368336554729737
2533912816378138240	38.54574127236897	-0.7804070255612395
2502056013151132416	39.118731742497225	0.974653322663511
2502081130120406528	39.236364631251	1.2163116816178396
2502078828017934976	316.90387037856755	1.2158615583852557
2689940182148617600	316.96756497949974	-0.2493725562698536
2690039619232587904	317.462892208272	0.22940114434322467
2689985949321335040	317.0053485392748	0.2871646537050567
2689936677455231232	317.49944867780863	-0.2937302157209761
2689965573995979648	317.160939656584	0.014718763352126166
2689942999647241344	0.2108166446454887	-0.20668902840093883
2738420570394779776	0.5500654944442763	1.1664309649524869
2738234340613251712	359.56440266357913	0.5481632616262625
2738290243907262336	359.41229766698933	0.7389542976573582
2738486850330373888	359.5625043039416	0.9654914155180373
2738265401816339968	359.2758973552364	0.5009792796684411
2738470323295882112	359.107371905424	0.6193875285768753
2738487915482214016	0.06323167674666405	0.7724502473856429
2738301415118440064	359.5725498692938	0.8092509964246917
2738289934669608832	0.2813896709186333	0.716411700437652
2738254578499203200	359.992560005623	0.6869801171078949
2738302682132584320	0.06142476687535918	0.8610583481650186
2738222349064557184	359.822688754111	0.5342482260360738
2738520625952901248	359.92647796746087	1.2001998718424933
2738196613620063872	359.95041491104115	0.2272931832203049
2738196338742153984	315.667598502849	0.20822262298004435
2690084046373203072	315.74954339329804	-0.22986572305122022

Table 6.39: Quasar candidates

Gaia ID	RA (deg)	DEC (deg)
2690169052367002368	316.63749627257965	0.19981302102374662
2690209223195939456	315.2245773439016	0.2853367961661892
2690158607006366720	315.3233208869523	0.1208711588108589
2690134623908412032	316.56198967080223	-0.0747263337004695
2690212861033010688	315.70056873822847	0.3500315512041742
2690091296278422912	56.03440355850458	-0.035479135122376194
3251545467209657344	57.114061740556046	-0.5182914809643779
3251298145811921664	55.3189418784827	-0.8343472531339317
3251442181835521024	56.61087857965463	-0.948321151578934
3251526397554074880	56.773958893583064	-0.4249071902719382
3251510935671806976	56.04646355187942	-0.4573468744424208
3251588279442753536	56.14984805907202	-0.2586713869587477
3251585496303945856	57.134925948683886	-0.2577002130868324
3251293232369325056	56.69214254867015	-0.9003144370402043
3251497638453212032	55.87346618143511	-0.7035732323843481
3251379406593102976	55.965218759474716	-1.1441153524841041
3251481523735510400	55.94132106322538	-0.8792080811505503
3251529627369235840	55.363421182990535	-0.800382477275268
3251404493498260736	56.18398068819689	-1.121884090471076
3251540381967766912	56.887379829479826	-0.6128913884255869
3251288559445239808	56.12112140532702	-0.9991709448944895
3251538423462290816	56.151046200372484	-0.6501728227752819
3251364911079613824	56.27070930993375	-1.1987644928132948
3251565533296287616	56.33679137909539	-0.49012589676372337
3251486785071728256	56.241805232209735	-0.8118900174428029
3251460358136993920	56.77978267701086	-1.0556268702624274
3251301547426353920	55.96674956673616	-0.9517133787413711
3251366212453556736	56.66082470942314	-1.2290867928890559
3251507710152368512	55.69684518945618	-0.6127307148967736
3251547288274900352	55.38031353604269	-0.6915741214465674
3251398476248212992	55.25307873977615	-1.2344682993282163
3251401362466236416	57.061529053089714	-1.2333584612574704
3251311687845498624	319.821364878231	-0.748529650132693
2686197135330631552	320.41015904630274	-1.247468083723237
2686167895193759104	321.4709182429472	-1.0922312922393267
2686097457729027840	320.36682240531997	-0.8030464640254852
2686165936687385344	321.0633140076535	-1.1583819296832685

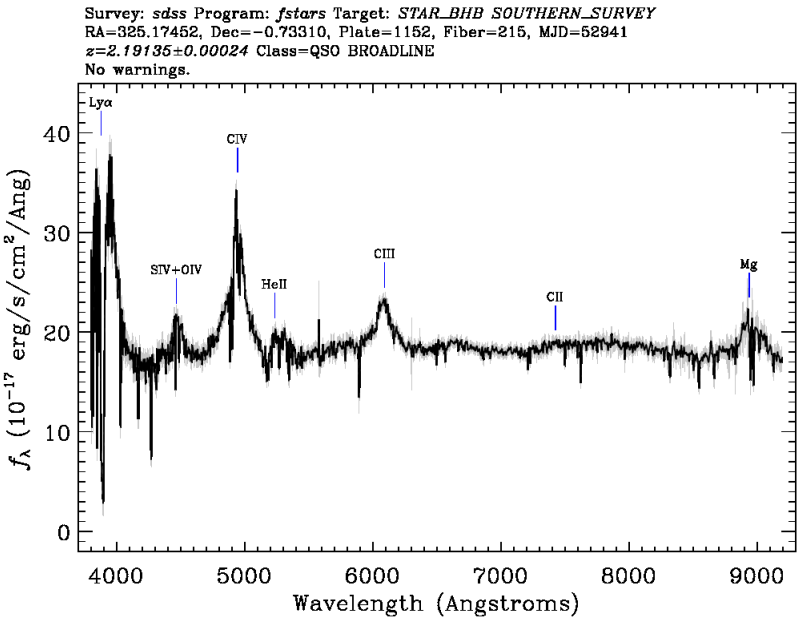

Figure 6.12: SDSS J230015.18+010520.0 spectra

Bibliography

[1] Eduardo Bañados, Bram P Venemans, Chiara Mazzucchelli, Emanuele P Farina, Fabian Walter, Feige Wang, Roberto Decarli, Daniel Stern, Xiaohui Fan, Frederick B Davies, et al. An 800-million-solar-mass black hole in a significantly neutral universe at a redshift of 7.5. *Nature*, 553(7689):473, 2018.

[2] Richard J Britto, E Bottacini, M Böttcher, DAH Buckley, S Buson, B Lott, JP Marais, PJ Meintjes, S Razzaque, and B van Soelen. Multi-wavelength study of fermi-lat blazars variability and radiation production mechanisms. *ApJ*, 565(773), 2002.

[3] DF Falla and MJ Floyd. Superluminal motion in astronomy. *European journal of physics*, 23(1):69, 2001.

[4] Robert P Fender, ST Garrington, DJ McKay, TWB Muxlow, Guy G Pooley, RE Spencer, AM Stirling, and EB Waltman. Merlin observations of relativistic ejections from grs 1915+ 105. *Monthly Notices of the Royal Astronomical Society*, 304(4):865–876, 1999.

[5] A Grazian, S Cristiani, V D'Odorico, A Omizzolo, and A Pizzella. The asiago-eso/rass qso survey. i. the catalog and the local qso luminosity function. *The Astronomical Journal*, 119(6):2540, 2000.

[6] Richard F Green, Marten Schmidt, and James Liebert. The palomar-green catalog of ultraviolet-excess stellar objects. *The Astrophysical Journal Supplement Series*, 61:305–352, 1986.

[7] Jesse L Greenstein and Maarten Schmidt. The quasi-stellar radio sources 3c 48 and 3c 273. *The Astrophysical Journal*, 140:1, 1964.

[8] KE Heintz, JPU Fynbo, E Høg, P Møller, J-K Krogager, S Geier, P Jakobsson, and L Christensen. Unidentified quasars among stationary objects from gaia dr2. *Astronomy & Astrophysics*, 615:L8, 2018.

[9] Karl G Jansky. A note on the source of interstellar interference. *Proceedings of the Institute of Radio Engineers*, 23(10):1158–1163, 1935.

[10] DAVID C Koo, RICHARD G Kron, and KYLE M Cudworth. Quasars to b¿ 22.5 in selected area 57: A catalog of multicolor photometry, variability and astrometry. *Publications of the Astronomical Society of the Pacific*, 98(601):285, 1986.

[11] Alan Thomas Koski. Spectrophotometry of seyfert 2 galaxies and narrow-line radio galaxies. *The Astrophysical Journal*, 223:56–73, 1978.

[12] J Low and DE Kleinmann. Proceedings of the conference on seyfert galaxies and related objects: 17. infrared observations of seyfert galaxies, quasistellar sources, and planetary nebulae. *The Astronomical Journal*, 73:868, 1968.

[13] Silvia Mateos, Almudena Alonso-Herrero, Francisco J Carrera, A Blain, Mike G Watson, Xavier Barcons, Valentina Braito, Paola Severgnini, Jennifer L Donley, and Daniel Stern. Using the bright ultrahard xmm–newton survey to define an ir selection of luminous agn based on wise colours. *Monthly Notices of the Royal Astronomical Society*, 426(4):3271–3281, 2012.

[14] Thomas A Matthews and Allan R Sandage. Optical identification of 3c 48, 3c 196, and 3c 286 with stellar objects. Technical report, OWENS VALLEY RADIO OBSERVATORY PASADENA CA, 1963.

[15] Patrick J McCarthy, Mark Dickinson, Alexei V Filippenko, Hyron Spinrad, and Wil JM van Breugel. Serendipitous discovery of a redshift 4.4 qso. *The Astrophysical Journal*, 328:L29–L33, 1988.

[16] Bradley M Peterson. *An introduction to active galactic nuclei*. Cambridge University Press, 1997.

[17] M Ryle and Allan Sandage. The optical identification of three new radio objects of the 3c 48 class. *The Astrophysical Journal*, 139:419, 1964.

[18] EE Salpeter. Accretion of interstellar matter by massive objects. *The Astrophysical Journal*, 140:796–800, 1964.

[19] Allan Sandage. The existence of a major new constituent of the universe: the quasistellar galaxies. *The Astrophysical Journal*, 141:1560, 1965.

[20] AR Sandage and DJK O'Connell. Study week on nuclei of galaxies. *ed. O'Connel, DJK, Elsevier, Nevy York*, page 271, 1971.

[21] Harlan J Smith and Dorrit Hoffleit. Light variations in the superluminous radio galaxy 3c273. *Nature*, 198(4881):650, 1963.

[22] LS Sparke and JS Gallagher. Galaxies in the universe (cambridge, 2000.

[23] Daniel Stern, Roberto J Assef, Dominic J Benford, Andrew Blain, Roc Cutri, Arjun Dey, Peter Eisenhardt, Roger L Griffith, TH Jarrett, Sean Lake, et al. Mid-infrared selection of active galactic nuclei with the wide-field infrared survey explorer. i. characterizing wise-selected active galactic nuclei in cosmos. *The Astrophysical Journal*, 753(1):30, 2012.

[24] PD Usher and KJ Mitchell. Variable quasi-stellar objects. ii-photometry and completeness of faint blue objects in the sandage-luyten survey field 15h 10m,+ 24 deg. *The Astrophysical Journal*, 223:1–12, 1978.

[25] AS Wilson and EJM Colbert. The origin of powerful radio sources. In *Bulletin of the American Astronomical Society*, volume 27, page 830, 1995.

[26] Edward L Wright, Peter RM Eisenhardt, Amy K Mainzer, Michael E Ressler, Roc M Cutri, Thomas Jarrett, J Davy Kirkpatrick, Deborah Padgett, Robert S McMillan, Michael Skrutskie, et al. The wide-field infrared survey explorer (wise): mission description and initial on-orbit performance. *The Astronomical Journal*, 140(6):1868, 2010.

[27] Nadia L Zakamska, Kelly Lampayan, Andreea Petric, Daniel Dicken, Jenny E Greene, Timothy M Heckman, Ryan C Hickox, Luis C Ho, Julian H Krolik, Nicole PH Nesvadba, et al. Star formation in quasar hosts and the origin of radio emission in radio-quiet quasars. *Monthly Notices of the Royal Astronomical Society*, 455(4):4191–4211, 2015.

[28] Ya B Zel'Dovich. The fate of a star and the evolution of gravitational energy upon accretion. *Accretion: A Collection of Influential Papers*, 5(3):57, 1989.